

MSE:
Transforming the Future of Engineering & IT



Arctic Wave Climate and Other Metocean Research at the University of Melbourne, Australia

Alexander Babanin

a.babanin@unimelb.edu.au

Сахалин, Россия
30 июля 2018



WIND-GENERATED WAVES, OCEAN and COASTAL ENGINEERING, AIR-SEA INTERACTIONS, OCEAN TURBULENCE, OCEAN DYNAMICS, CLIMATE, REMOTE SENSING

- **dynamics of surface ocean waves**
 - **wave breaking and dissipation**
- **spectral and phase-resolving modelling of the wind-generated waves**
 - **extreme waves**
 - **wave statistics**
- **wave-bottom interactions**
- **wave-current interactions**
 - **air-sea boundary layer**
 - **air-sea interactions**
 - **ocean turbulence**
 - **ocean mixing**
 - **wave climate**
 - **climate change**
 - **extreme oceanic conditions**
- **environmental measurements and instrumentation**
 - **ocean remote sensing**





swell



deep water



rogue waves



extreme conditions



finite depth



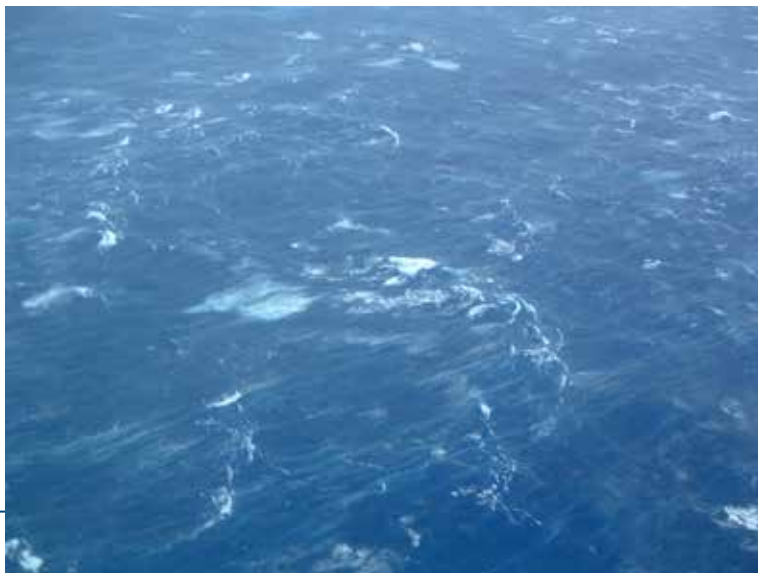
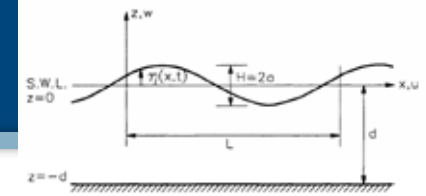
waves on currents



ice



directional waves

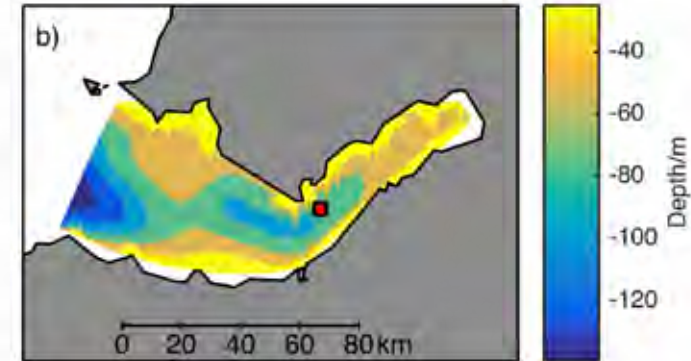
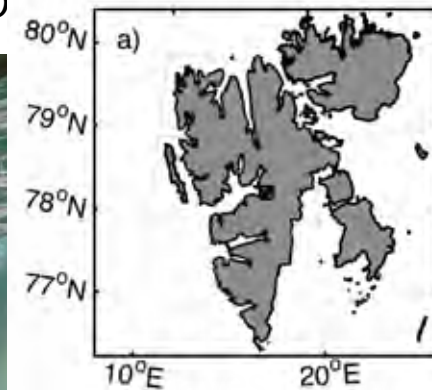
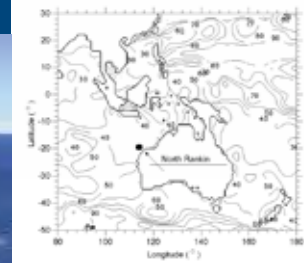


Facilities and experiments

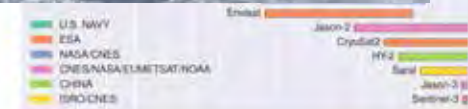
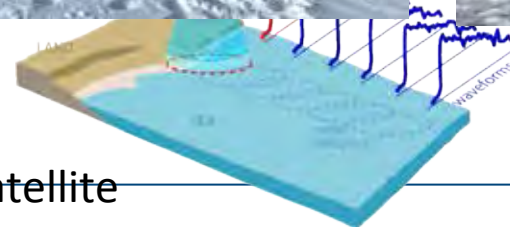
(c) Windtunnel



- Extreme wind-wave flume
- winds up to 70 m/s (Cat.5 TC)
- Wavemaker
- to



• V
tem

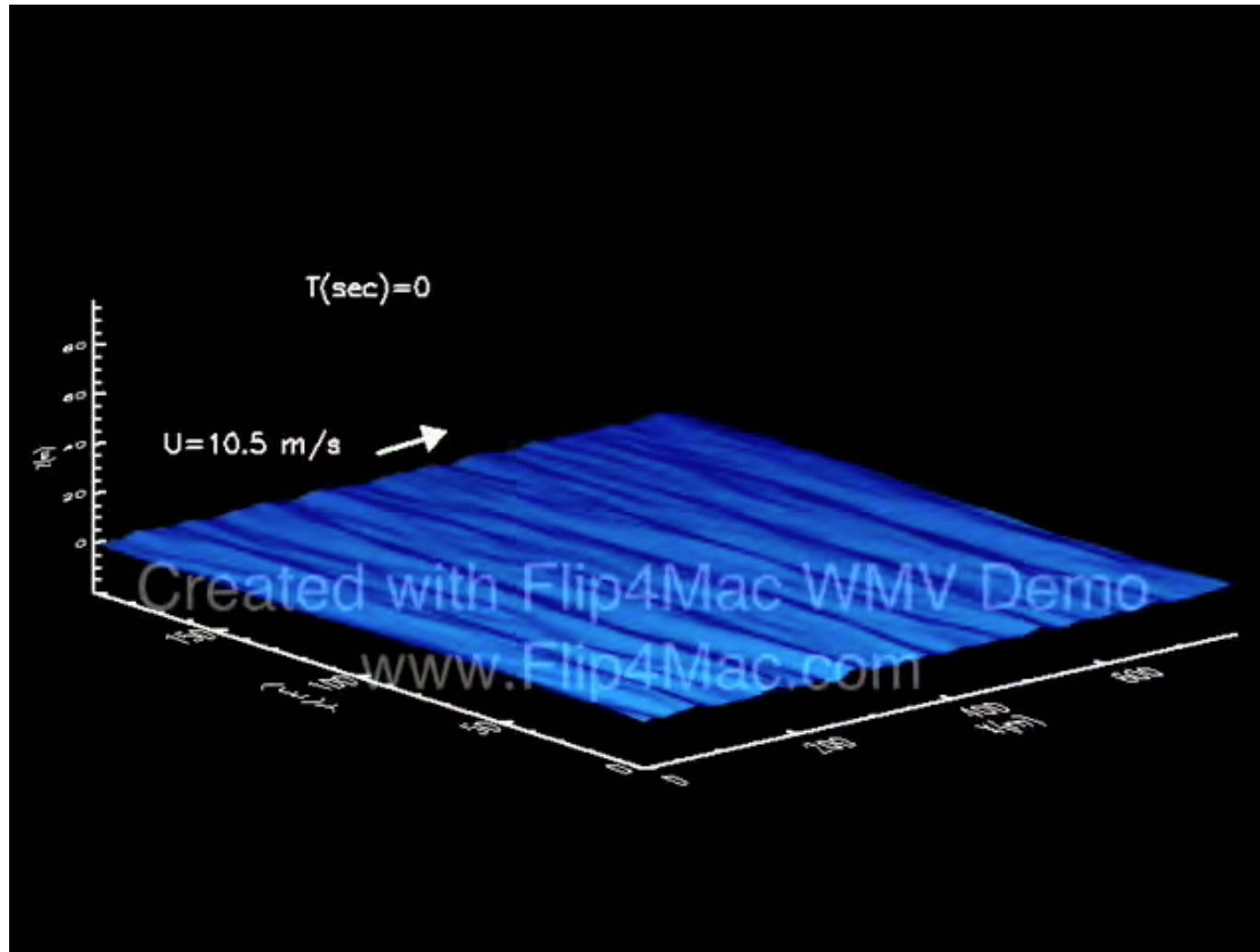


Global satellite database, 30 years



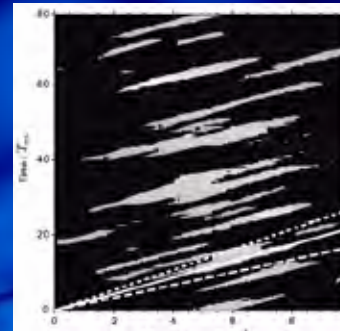
phase resolving modelling

- state of the art models
 - explicit simulations of surface elevations, turbulent wind, underwater kinematics and dynamics
-



engineering problems: breaking probability, short-crestedness, kinematics
Chalikov & Babanin, *OMAE*, 2013

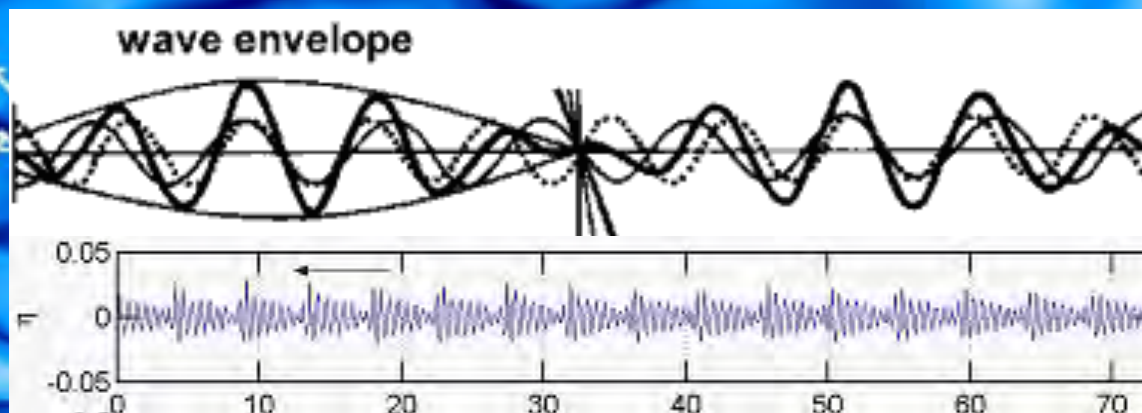
*Nieto Borge et al.,
OM, 2013*



1/128 of total domain

2D freak wave appearance

freak wave, $H = 2H_s$



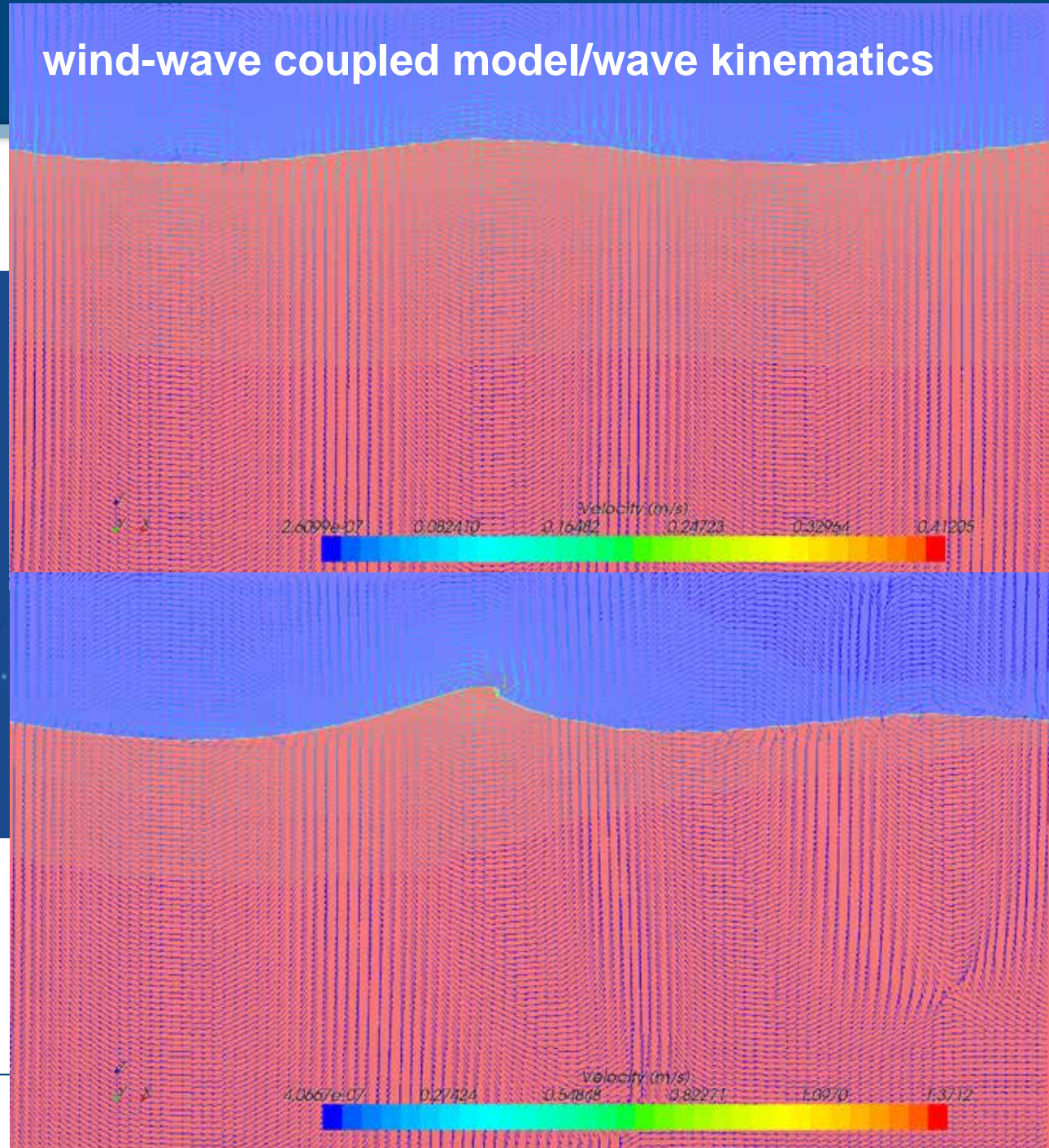


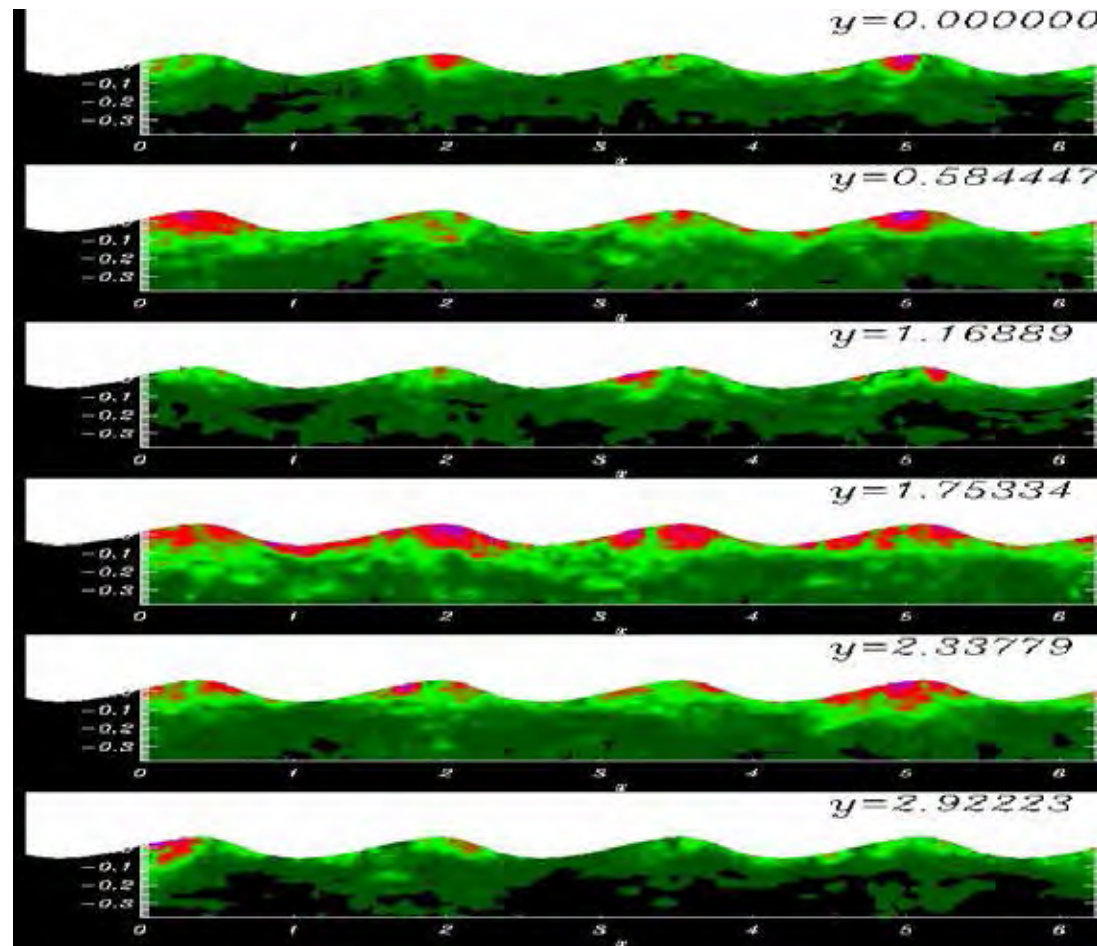
Chalikov & Rainchik,
BLM, 2011

Created with Flip4Mac
www.Flip4Mac.com

Chabchoub et al., *OMAE*,
2014

wind-wave coupled model/wave kinematics





based on first principles
newly described phenomenon

Babanin & Chalikov, *JGR*, 2012



$$\frac{dE(k, f, \theta, x, t)}{dt} = S_{tot} = S_{in} + S_{ds} + S_{nl} + S_{bf}$$

spectral wave modelling

- new release of official models used for wave forecast, ocean/coastal engineering
-

Wind Input, following the waves



$$\frac{dE(k, f, \theta, x, t)}{dt} = S_{tot} = S_{in} + S_{ds} + S_{nl} + S_{bf}$$

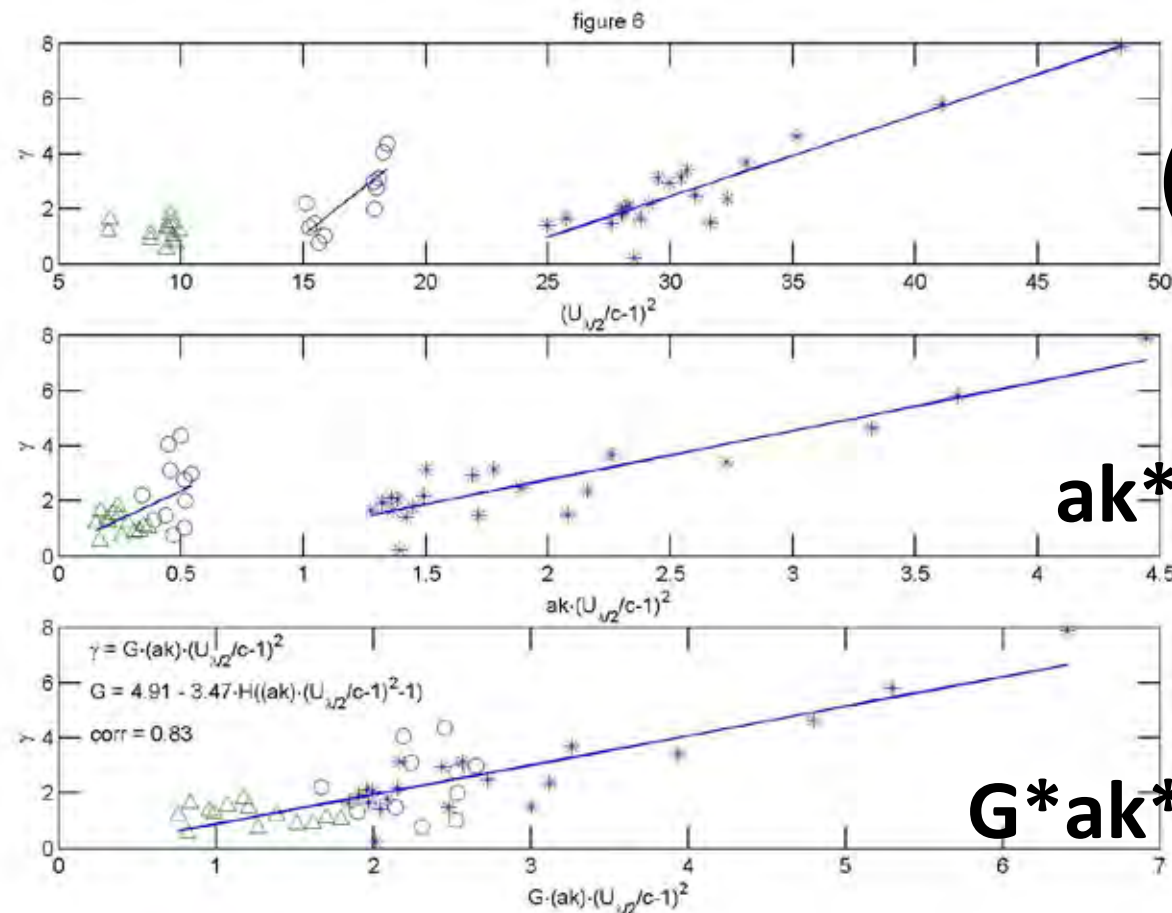


Young et al., JAOT, 2005, Donelan et al., JAOT, 2005, JPO, 2006, Babanin et al., JPO, 2007



$$\frac{dE(k, f, \theta, x, t)}{dt} = S_{tot} = S_{in} + S_{ds} + S_{nl} + S_{bf}$$

The parameterisation, growth rate γ



$$(U/c-1)^2$$

$$ak \cdot (U/c-1)^2$$

$$G \cdot ak \cdot (U/c-1)^2$$

$$S_{in}(\omega) = \rho_a \omega g \gamma(\omega) E(\omega)$$



Observation-based physics

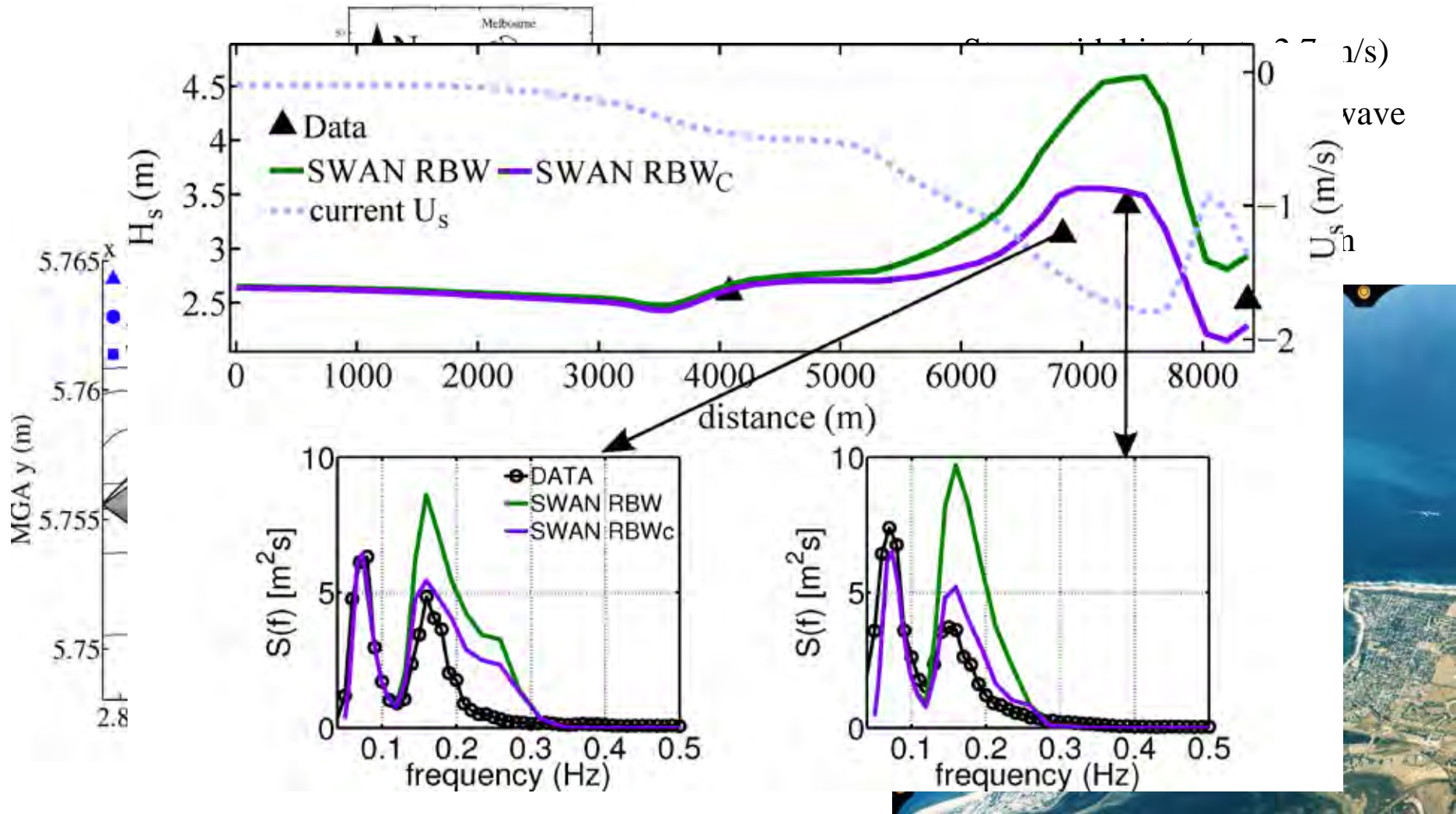
$$\frac{dE(k, f, \theta, x, t)}{dt} = S_{tot} = S_{in} + S_{ds} + S_{nl} + S_{bf}$$

- replaced previous physics
- implemented in official releases of WAVEWATCH-III (US NOAA wave-forecast model), SWAN (European coastal engineering model) – both used internationally
- new source terms: wind input, whitecapping dissipation, swell dissipation, wave-bottom interaction, interaction with adverse winds
- quantitatively: based on measurements
- qualitatively: new physical features, previously unknown
- in progress: nonlinear wave-current interactions, nonlinear wave-wave interactions, coupling with phase-resolving models, wave-ice modules, infragravity waves, directional source functions

Current-induced dissipation – Port Phillip Heads

MELBOURNE

Strong wave dissipation on the tidal jet



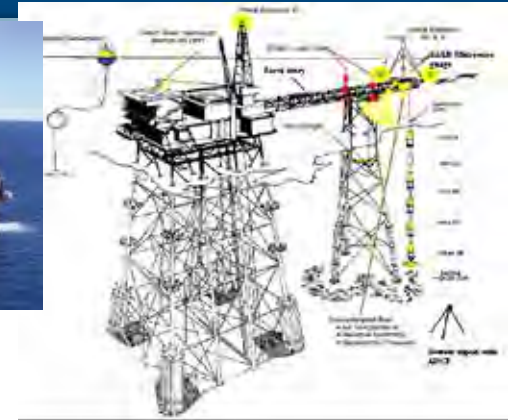
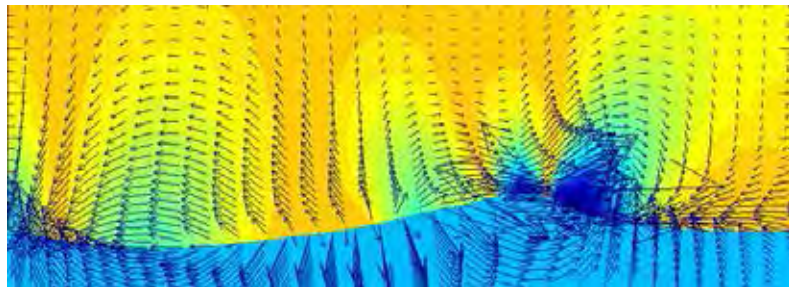
Source: Port of Melbourne Corporation

Rapizo et al., *JGR*, 2017

- At wind speeds $U_{10} > 32 \text{ m/s}$, dynamics of the atmospheric boundary layer, of the ocean wave surface and of the upper ocean layer – all change
 - At the surface, at $U_{10} \sim 34 \text{ m/s}$:
 - wave asymmetry saturates
 - mass transfer velocity and volume flux of droplets increase sharply
 - This indicates change of the wave breaking mechanism to the direct wind forcing
 - Sea drag saturates at $U_{10} = 32\text{-}33 \text{ m/s}$ above the surface
 - Cross-interface gas fluxes still grow, but at a slow rate if $U_{10} > 35 \text{ m/s}$, additional mechanisms become active below the surface
 - ***Simultaneous change of the regime in all the three air-sea environments can hardly be coincidental***
-
- ***It is likely that wave breaking is responsible for that***



Chalikov & Rainchik, BLM, 2011



SEPTEMBER 2011

TOFFOLI ET AL.

1179

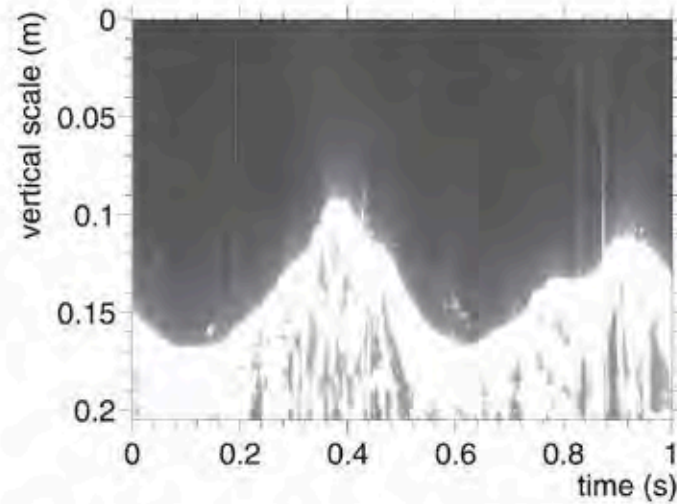


FIG. 2. Sample image from the digital line scan camera: $U_{10} = 30 \text{ m s}^{-1}$. The image is composed by 250 line scans stacked into a 1-s image.

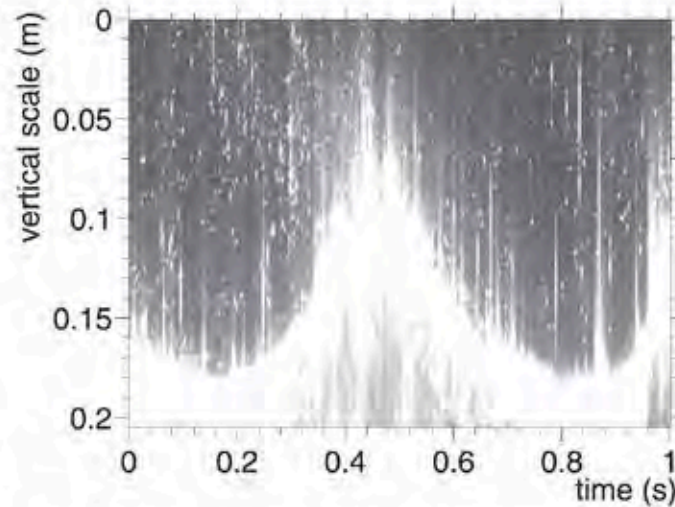


FIG. 3. Sample image from the digital line scan camera: $U_{10} = 60 \text{ m s}^{-1}$. The image is composed by 250 line scans stacked into a 1-s image.

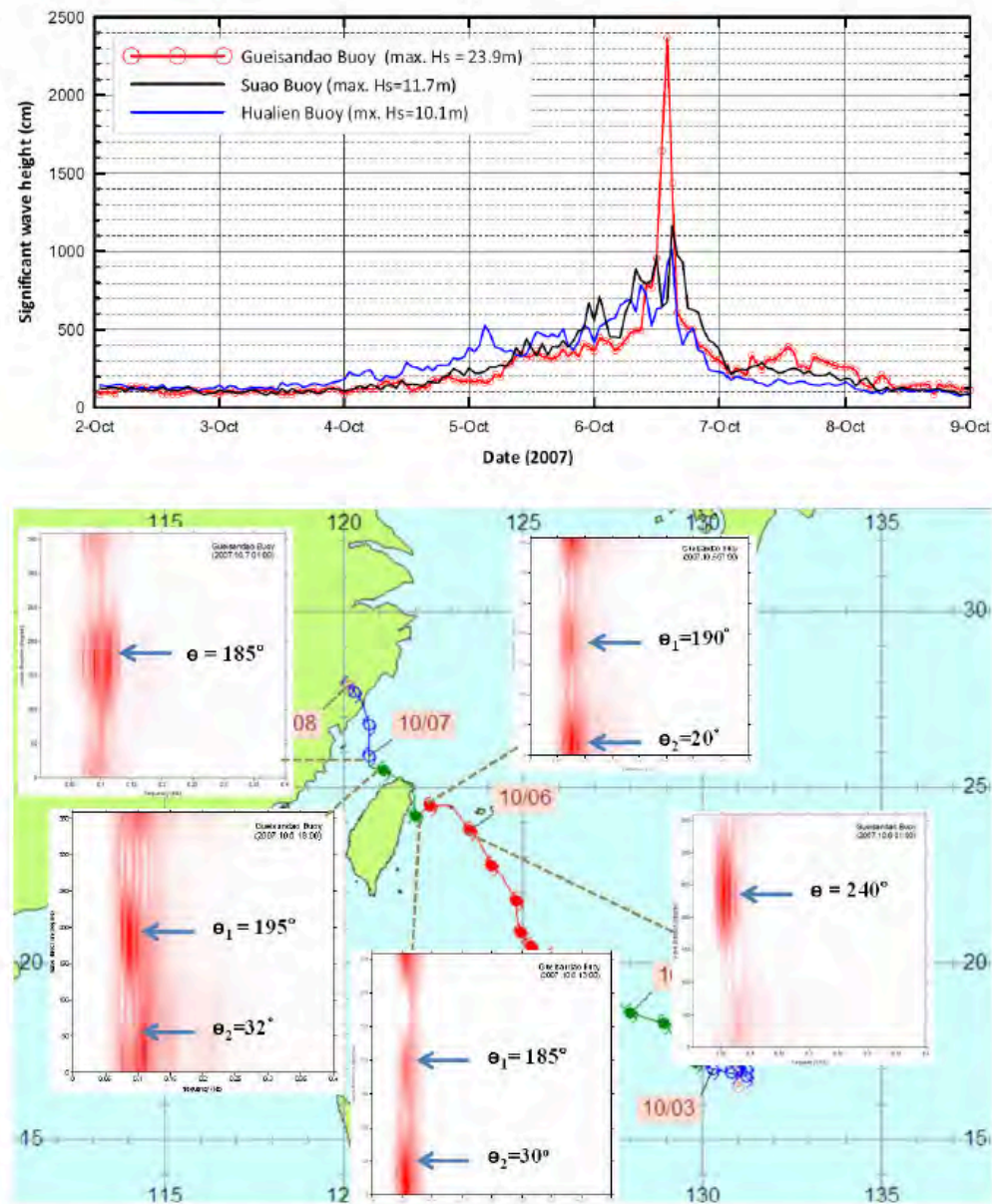
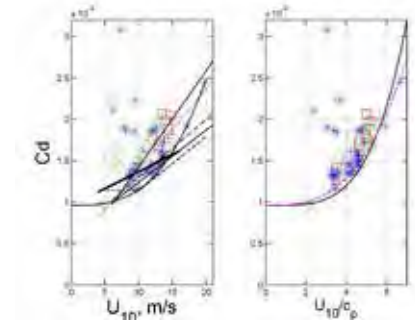


Fig. 3. Top: significant wave height recorded on hourly basis between 2 and 9 October at the Guishandao, Suao and Hualien Buoys. Bottom: directional wave spectra during Typhoon Krosa.



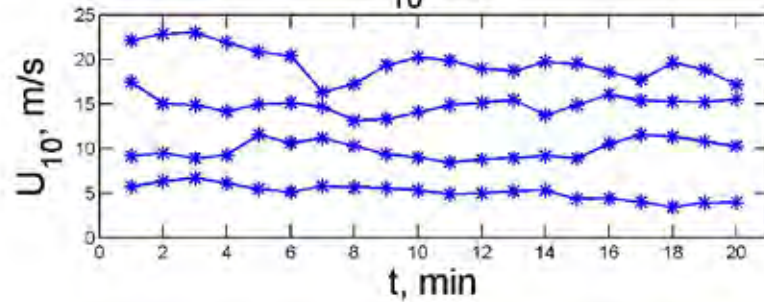
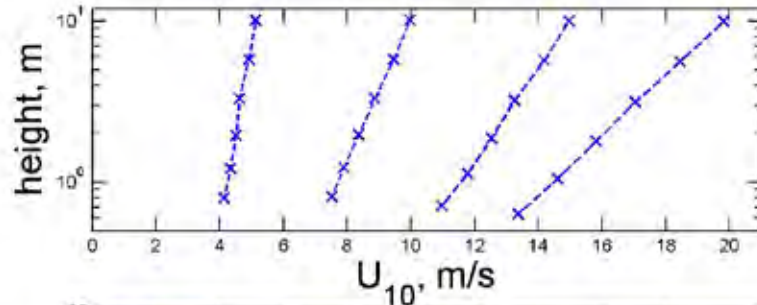
sea drag

$$\tau = \rho_a \text{mean}(u'w') = \rho_a u_*^2 = \rho_a C_d U_{10}^2$$

- in every air-sea interaction model
- intends to replace the physics of the boundary layer with a single coefficient, dependent on the wind
- dependences on wind forcing, gustiness, wave spectrum, breaking, nonlinearity, flow separation, air humidity are investigated



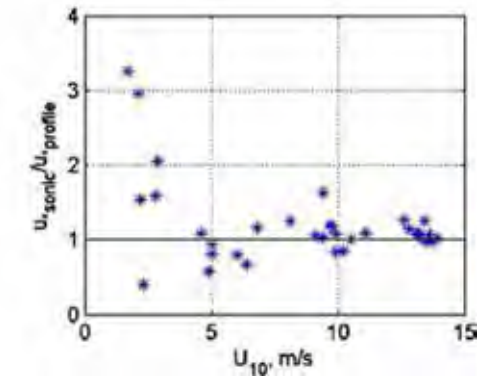
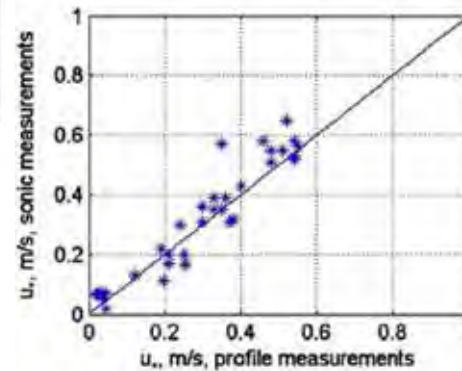
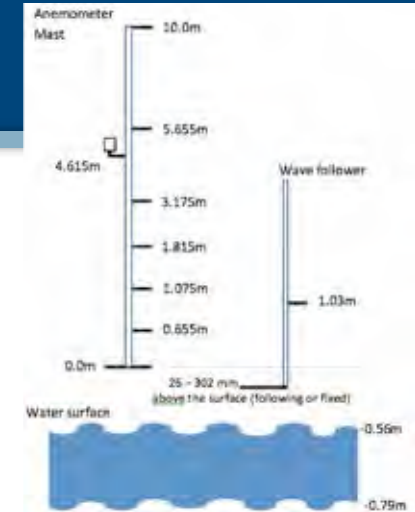
ABL measurements



$$\tau = \rho_a u_*^2 = \rho_a \overline{u'w'} = \rho_a C_d U_{10}^2$$

$$U(z) = \frac{u_*}{K} \ln \frac{z}{z_0}$$

- inter-comparisons were done with Sonic anemometer
- light winds $U_{10} < 4\text{m/s}$ were excluded from analysis

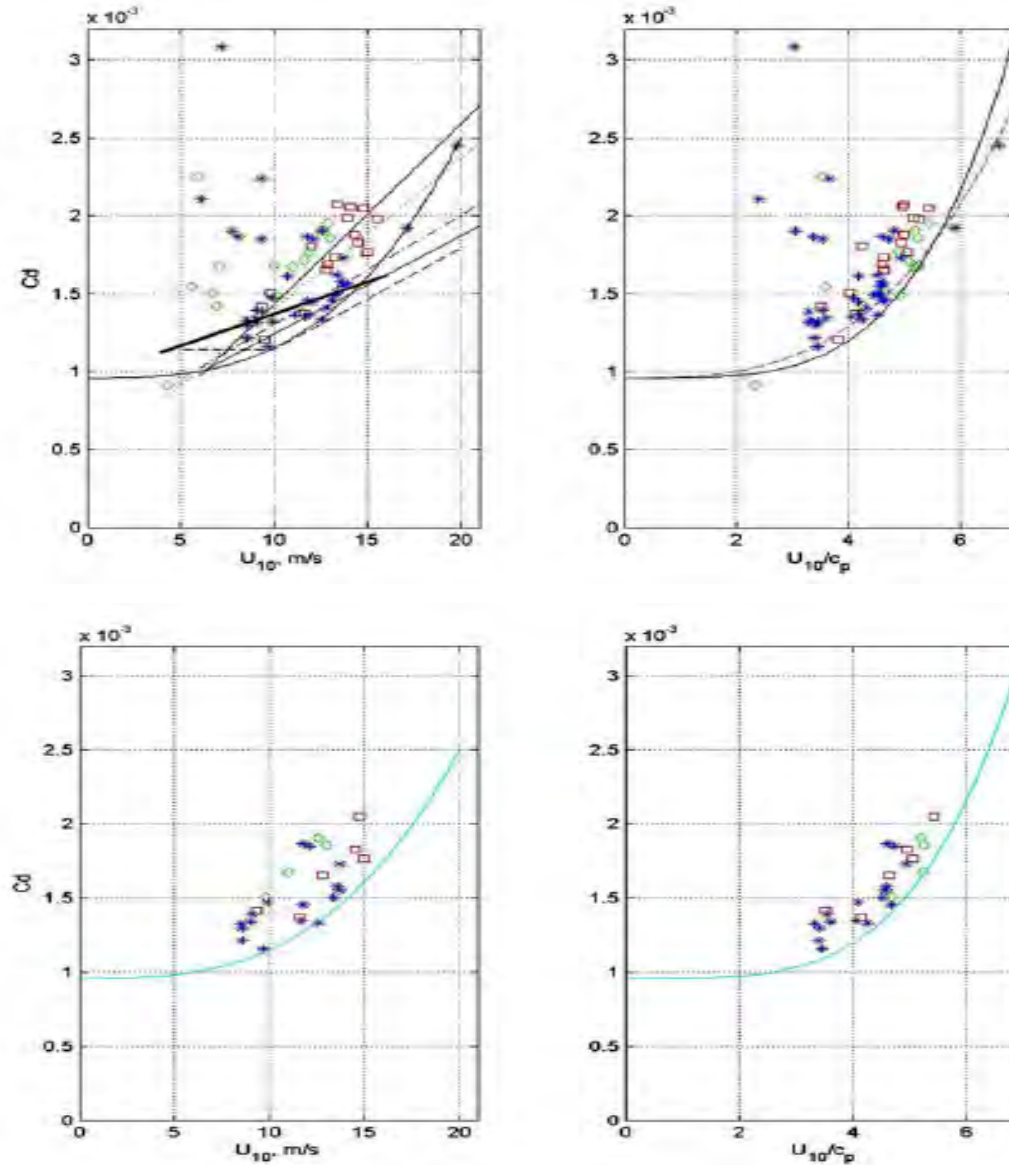




C02015

BABANIN AND MAKIN: WIND TREND AND GUSTINESS ON SEA DRAG

C02015





Toffoli, Loffredo, Le Roy, Lefevre, Babanin, JGR, 2012

$$\mu = \frac{1}{2}a \left\{ \frac{k[4 \tanh(kh) + \tanh(2kh)][1 - \tanh(kh)^2]}{\tanh(kh)[2 \tanh(kh) - \tanh(2kh)]} + 2k \tanh(kh) \right\},$$

125

TOFFOLI ET AL.: VARIABILITY OF SEA DRAG

C0

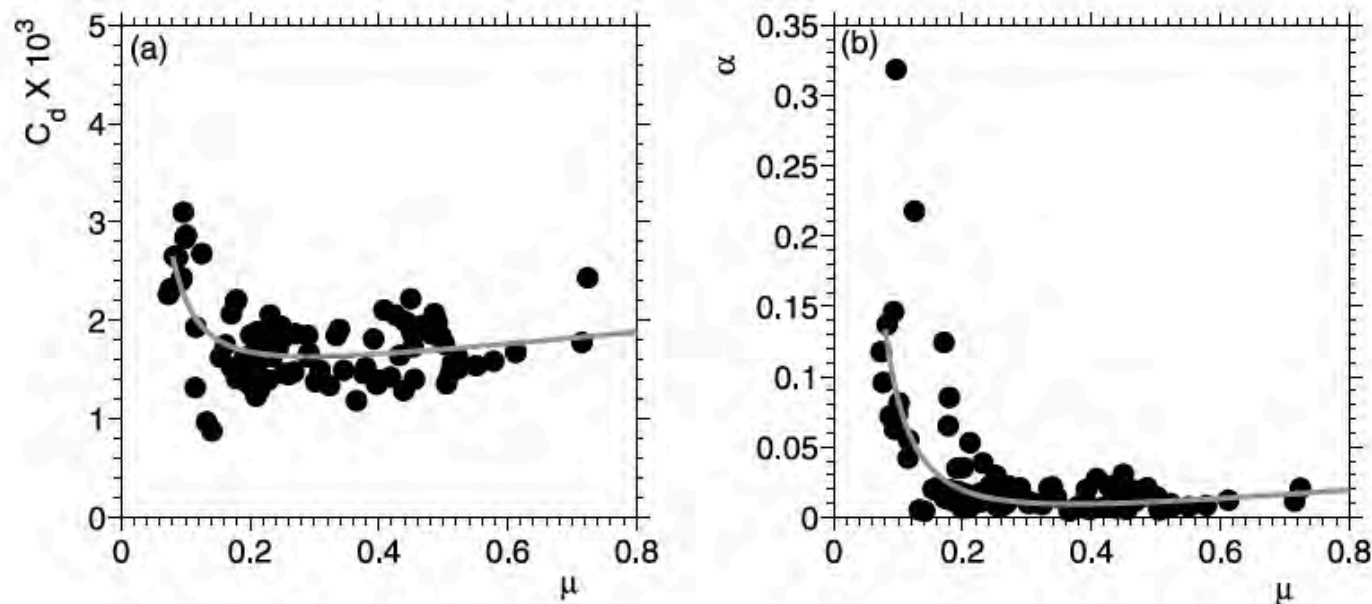
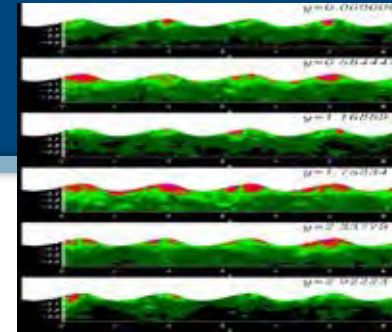
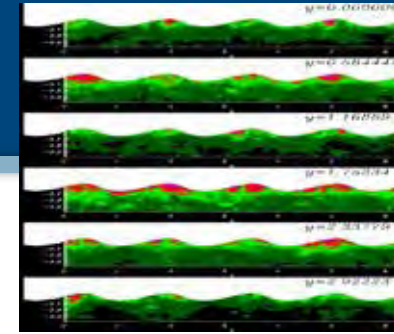


Figure 6. (a) Sea drag and (b) Charnock coefficient dependence on the general nonlinear parameter μ ; regression lines have the following form: $C_d = 0.01\mu^{-2} + 0.65\mu + 1.35$ (Figure 6a); $\alpha = 0.001\mu^{-2} + 0.03\mu - 0.01$ (Figure 6b).



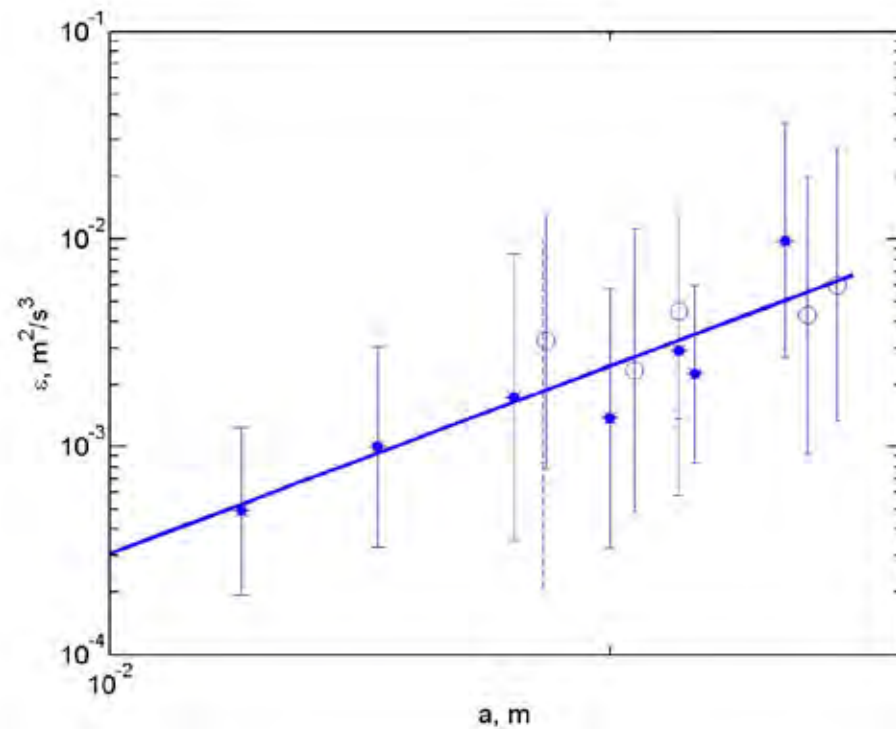
wave mixing in the upper ocean

- new research field
 - sediment suspension, tropical cyclones, weather, climate
-

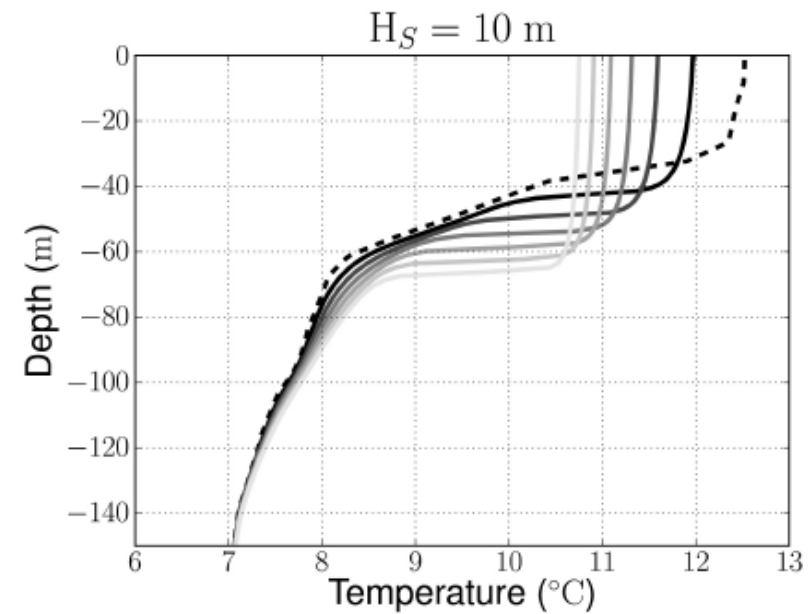


Laboratory experiments and numerical simulations

$$\varepsilon = 300 \cdot a^{3.0 \pm 1.0}$$



Babanin & Haus, *JPO*, 2009

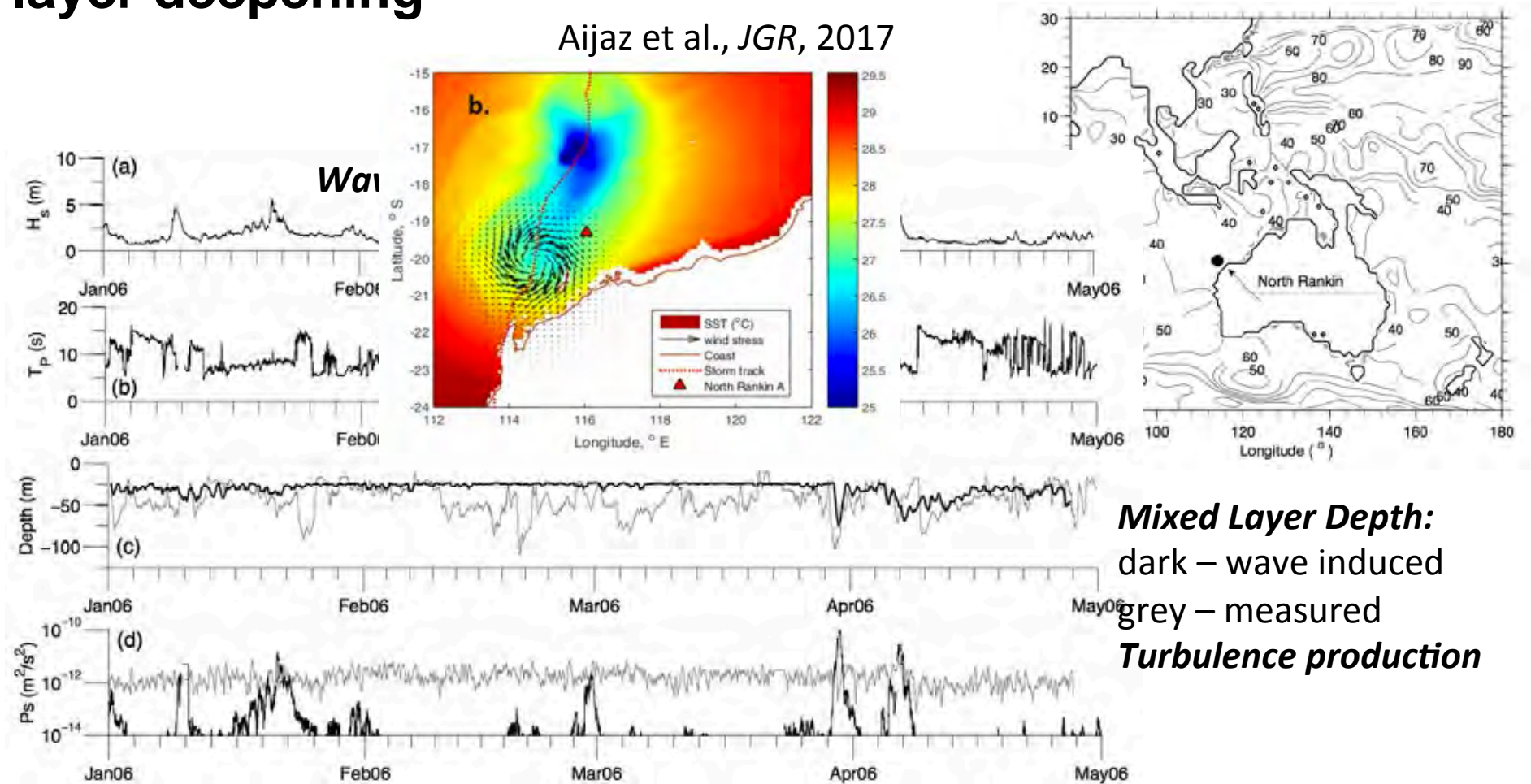


Ghantous & Babanin, *NPG*, 2014



Field observations, North Rankin mixed layer deepening

Aijaz et al., *JGR*, 2017



Toffoli et al., *JGR*, 2012



Pleskachevsky et al., *JPO*, 2011

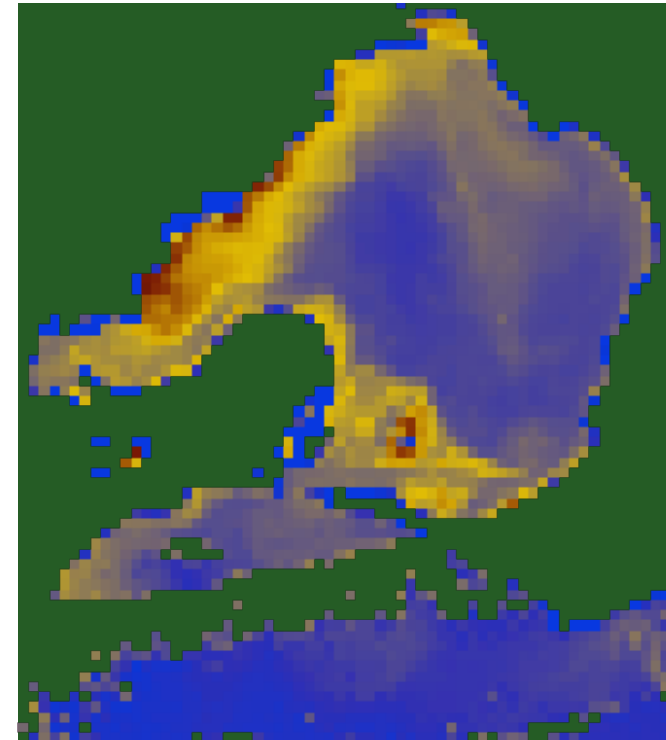
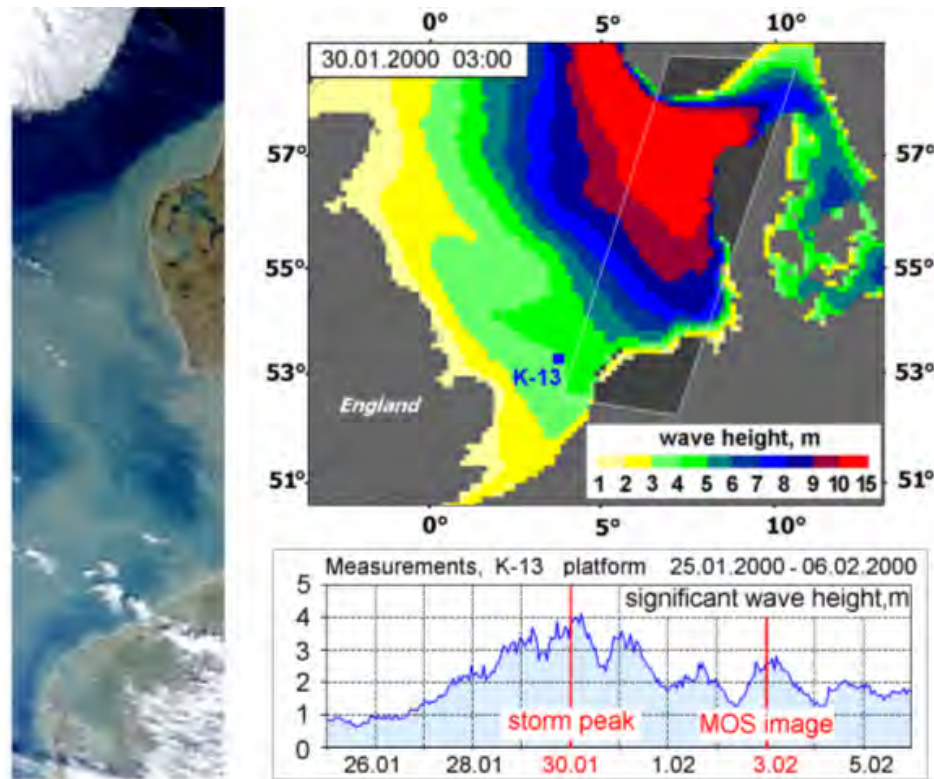


FIG. 1. Storm events in the North Sea at 29.01-04.02.2000 (the storm peak on 30.01.2000, at about 03:00 UTC). Optical MOS image of German Bight on 03.02.2000 (left) and significant wave height in the North Sea at the storm peak (right).

field observations and modelling, North Sea (left), Port Phillip (right)



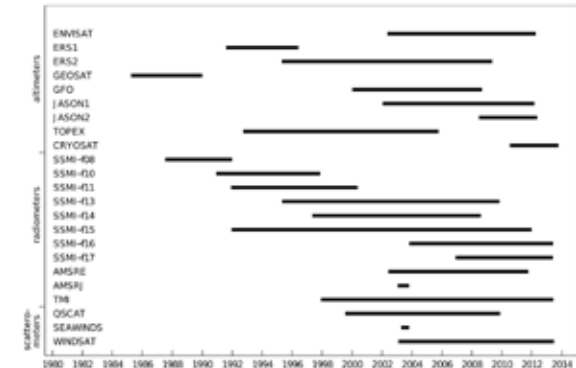
global wind/wave climate

- new research field
 - satellite observations provide information on metocean properties globally, over ~30 years
 - waves can also serve as a climate proxy, and influence the atmospheric and oceanic climate
-

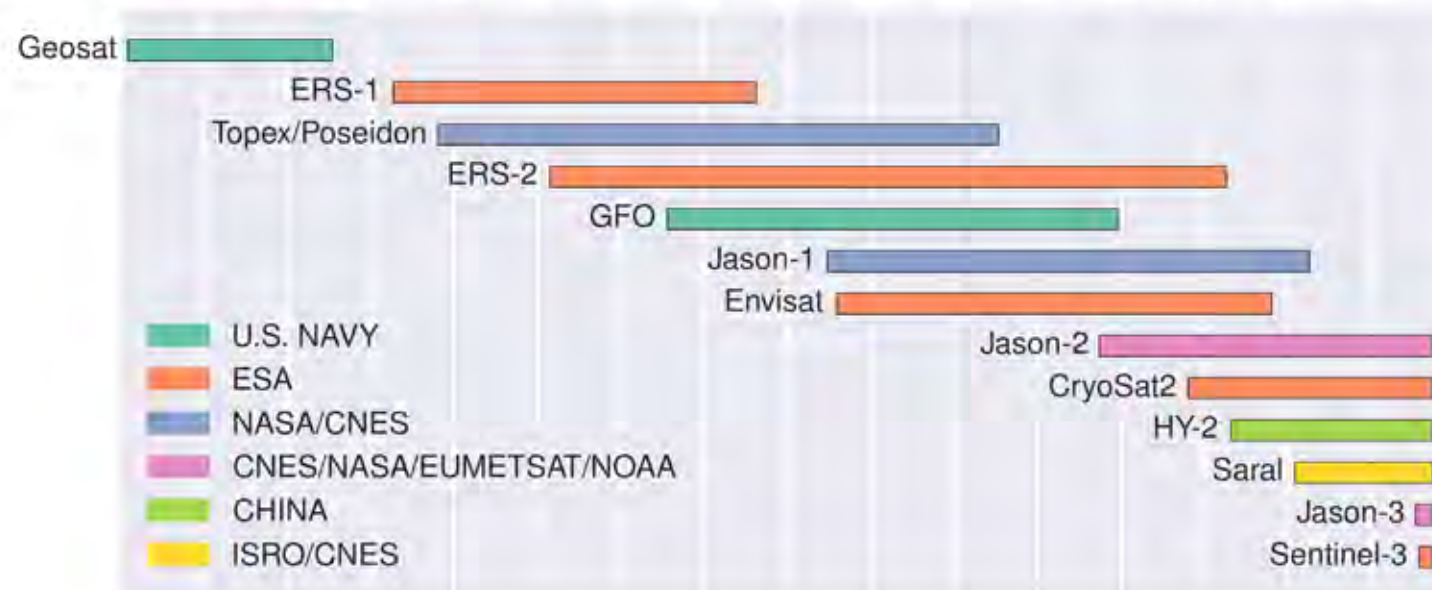


Altimeter and other Metocean Data

- Continuous satellite global coverage since 1991
- ERS1 , ERS2 and ENVISAT cover up to 82° lat.
- GEOSAT and GFO cover up to 72° latitude
- JASON and TOPEX reach 66° latitude
- JASON and TOPEX reach 66° latitude
- CRYOSAT2 covers areas up to 88°
- HY-2 covers areas up to 80°
- SARAL covers areas up to 81°



Year 85 87 89 91 93 95 97 99 01 03 05 07 09 11 13 15 17

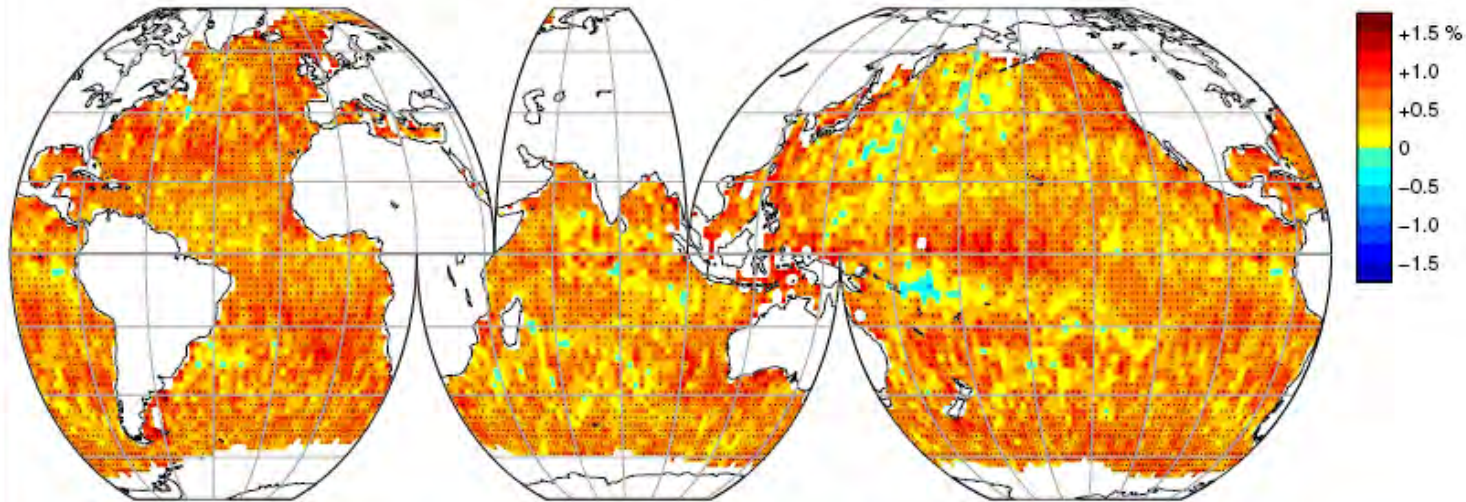


Global measurements of waves, winds, currents, ice, sea surface temperature, among other metocean properties

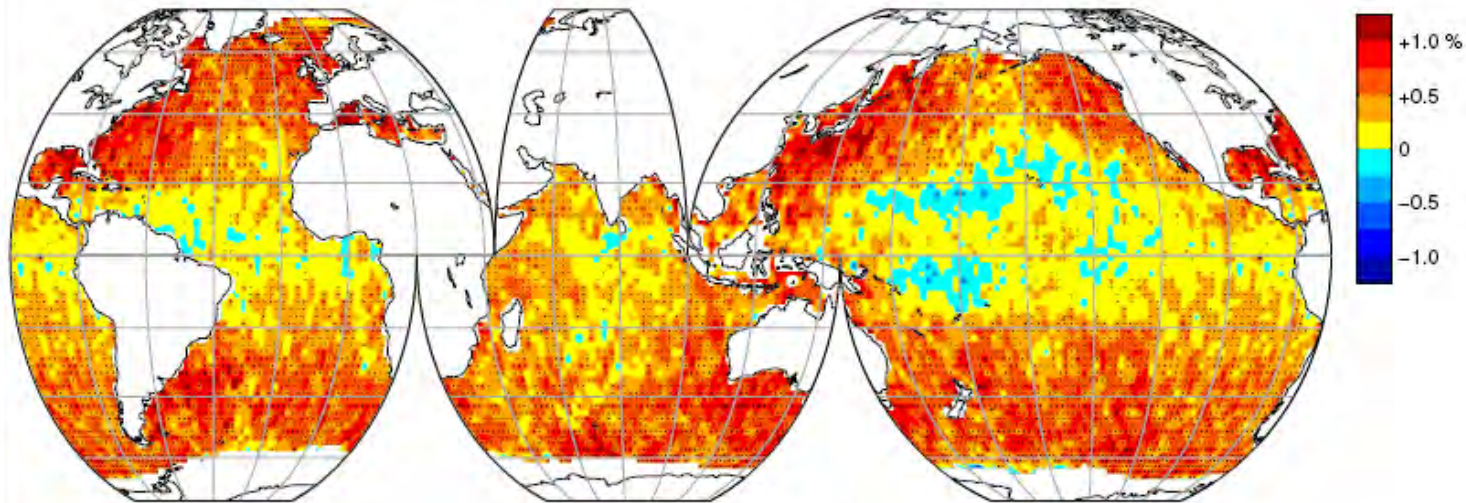


satellite observations, global wind and wave trends, 25 years

99th percentile wind speed (1991–2008)



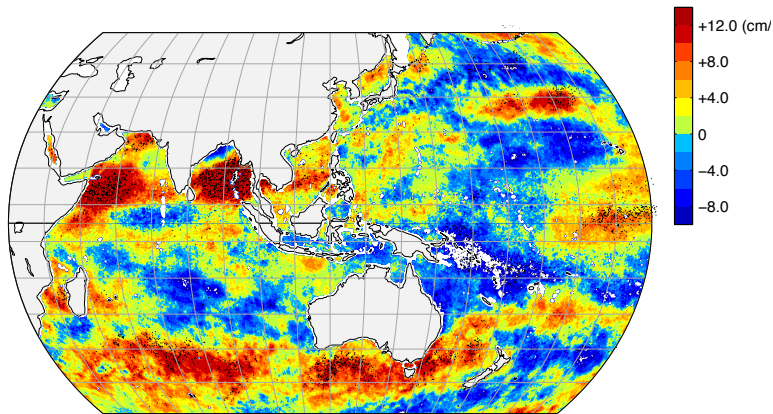
99th percentile significant wave height (1985–2008)





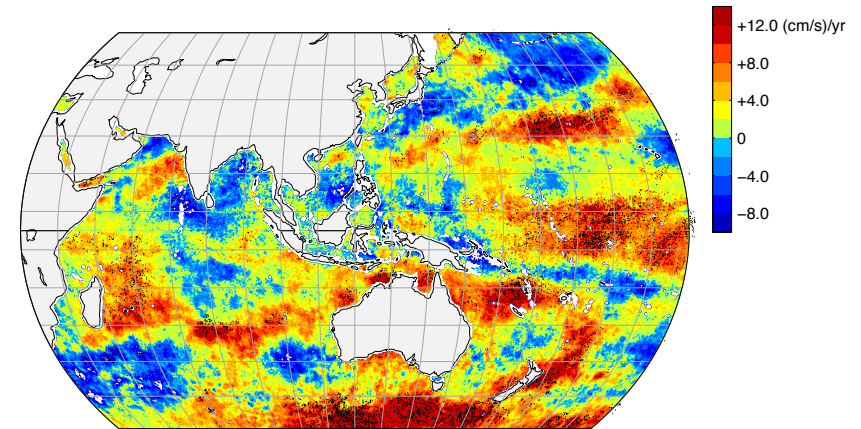
Wind Trends, by SSM/I

mean wind speed (May 1991–2008)



Trend analysis (MK test) applied to monthly mean SSM/I (F10,F11,F13) wind and precipitation from 1991 to 2008. Hatching indicates significant changes (normcdf test [95% level]) and contour interval is 2.00 cm s^{-1} per year.

mean wind speed (Jun 1991–2008)



Trend analysis (MK test) applied to monthly mean SSM/I (F10,F11,F13) wind and precipitation from 1991 to 2008. Hatching indicates significant changes (normcdf test [95% level]) and contour interval is 2.00 cm s^{-1} per year.



THE UNIVERSITY OF
MELBOURNE

Arctic Research at the University of Melbourne

- Sea ice has been retreating in summer months in the Arctic
 - Waves become an issue: navigation, air-sea interactions, coastal erosion etc.
 - Wave climate and trends are unknown
 - Wave modelling is problematic
 - Satellite-borne devices can measure the global wind, wave and other climate properties with global coverage and accuracy comparable to buoy observations
-

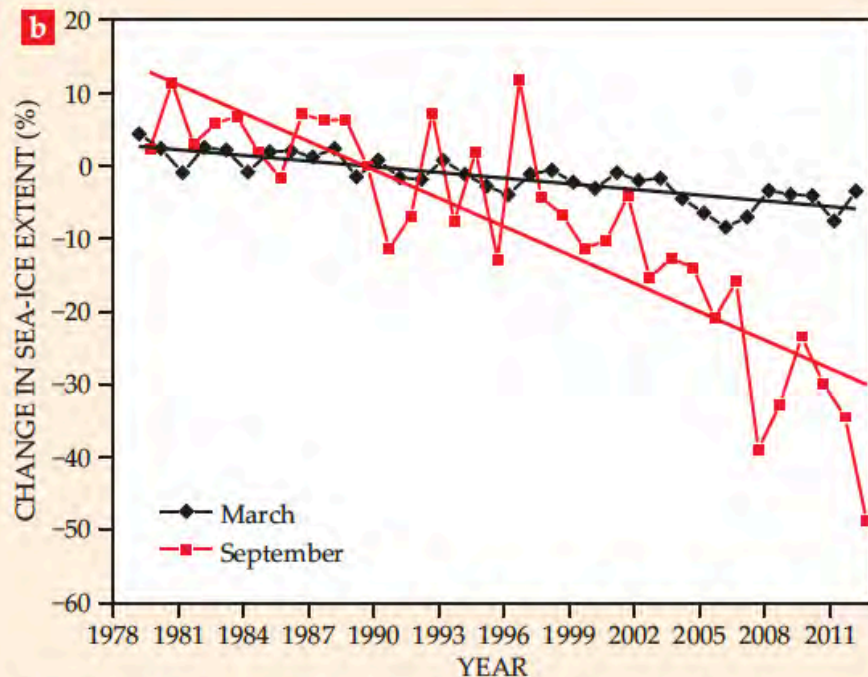


Figure 2. The decline in areal extent of Arctic sea ice has been mapped daily since 1979 by satellites using passive microwave sensors. (a) Between September 1980, when the summer minimum was 7.5 million square kilometers, and September 2012, when there were 3.4 million square kilometers of ice, the end of summer ice extent has shrunk by 55%. (b) Minimum (September) and maximum (March) ice-extent anomalies for each year are plotted beginning in 1979, when satellite observations began. Each data point represents the departure of the measured ice extent in March and September each year from the average of those months over the reference period 1979–2012. (Data are from the Sea Ice Index, National Snow and Ice Data Center; see http://nsidc.org/data/seaice_index. Walt Meier provided the plot.)

The Arctic

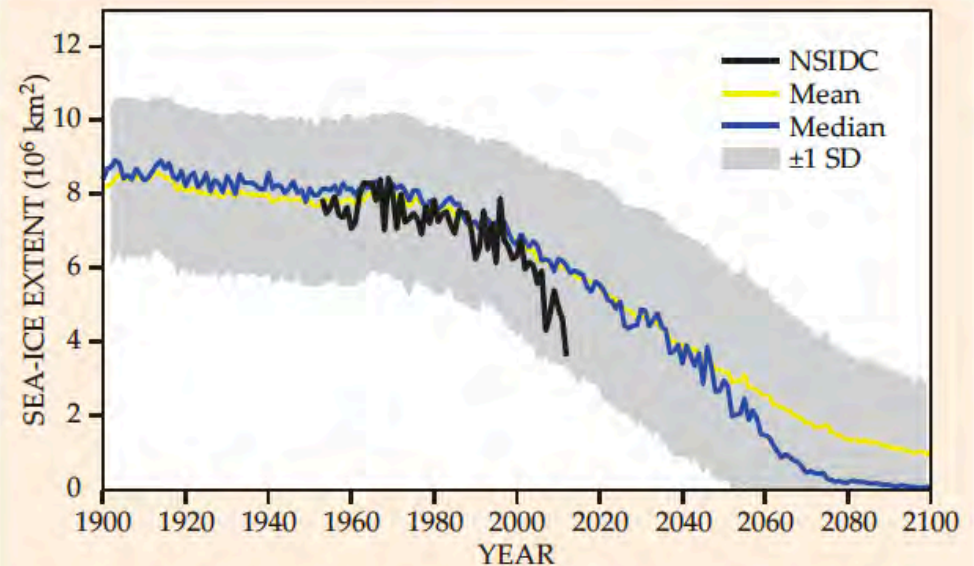


Figure 6. Sea-ice extent is declining faster than models predict.

The large spread of ± 1 standard deviation (SD; gray) in 84 predictions of ice extent from 36 different current models underscores the uncertainty about the future state of the ice cover and the need to improve our understanding of air-ice-ocean processes and their representation in the models. These and similar results form the basis for the fifth assessment report of the Intergovernmental Panel on Climate Change. The black curve plots observational data dating back to 1953 from the National Snow and Ice Data Center (NSIDC). The yellow and blue curves are the mean and median of the model results, respectively. (Adapted from ref. 13.)



Satellite Observations of Metocean Properties in the Arctic Ocean

following Liu, Q., A.V. Babanin, S. Zieger, I.R. Young, and C. Guan, 2016: Wind and wave climate in the Arctic Ocean as observed by altimeters. *Journal of Climate*, 29, 7957-7975



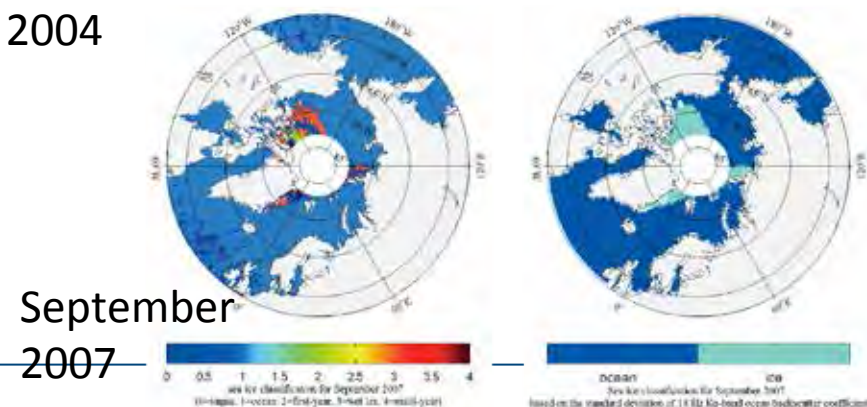
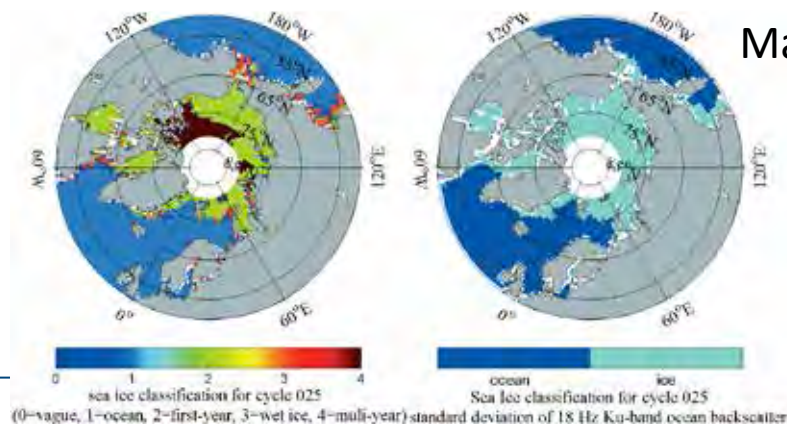
Recap

- Globally, waves and winds have been growing
 - Extremes grow faster than mean values
 - Ice has been retreating in the Arctic summers since 2005 (?)
 - Notably, not in Antarctic
 - At high latitudes, winds have been shifting polarwards
 - What about the waves at high latitudes?
-



- The altimetry data are available since mid 80s
 - Altimeters can estimate wave height about every second over a footprint of 1-10km
 - Satellite altimetry is also able to provide information on surface winds, concentration and other properties of ice, on storm events, and on the respective trends in these quantities
 - Altimeters of the European Space Agency cover up to the 80th degree north/south and higher
 - *Problem:* invalid measurements must be removed first – land, rain, ice
-

- needs to be based on altimeter measurements
- Tran et al. (2009) suggested a three-parameter cluster algorithm to brightness temperature data and backscatter data
- brightness data are not always available
- Laxon (1990) and Rinne and Skourup (2012) approach is a one-parameter classification algorithm

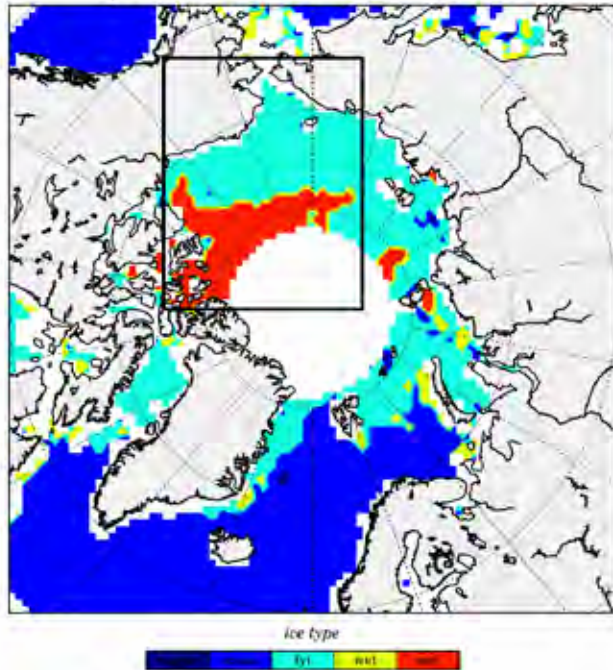




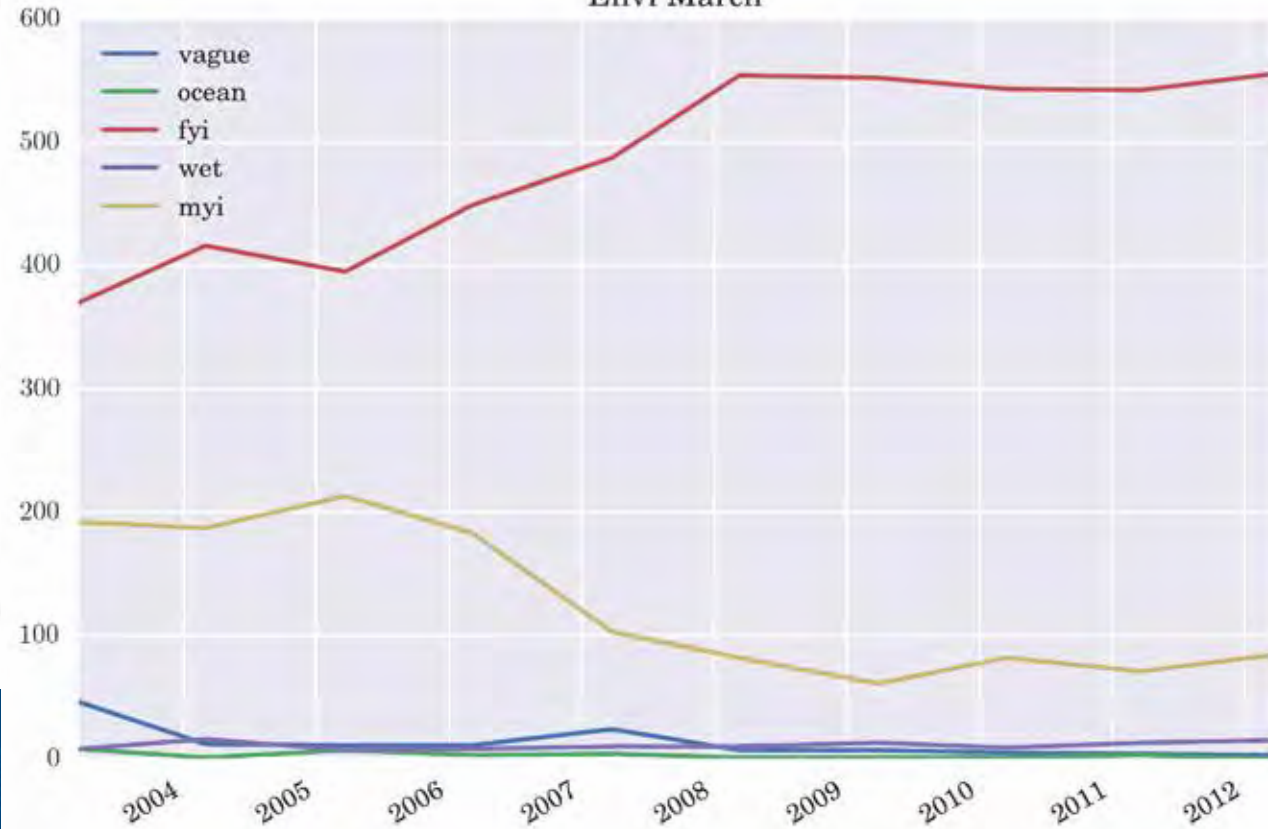
Ice trends



Cycle 025 - Envisat ICE - Apr 2004

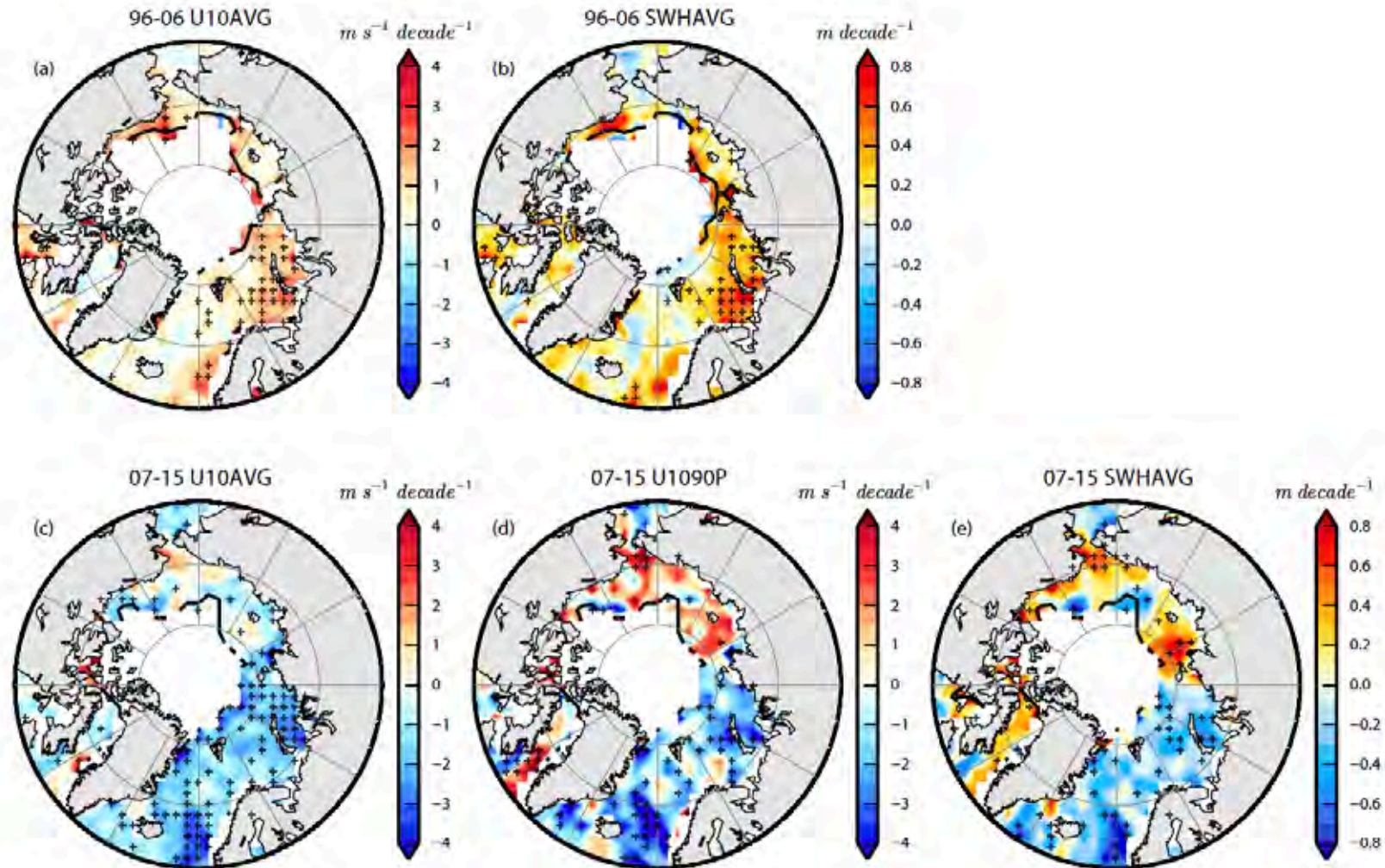


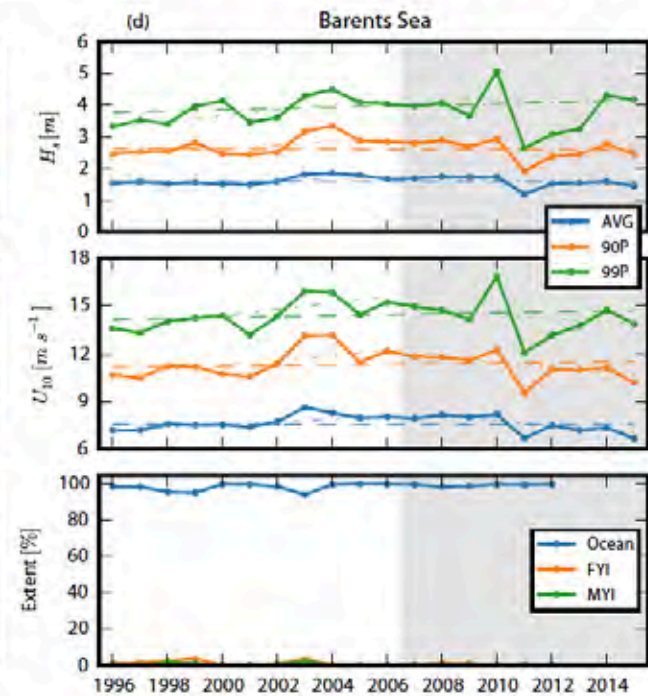
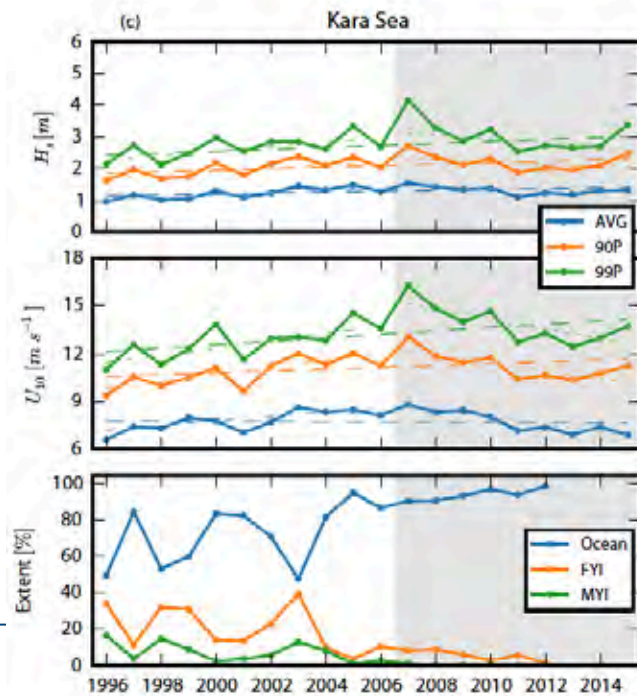
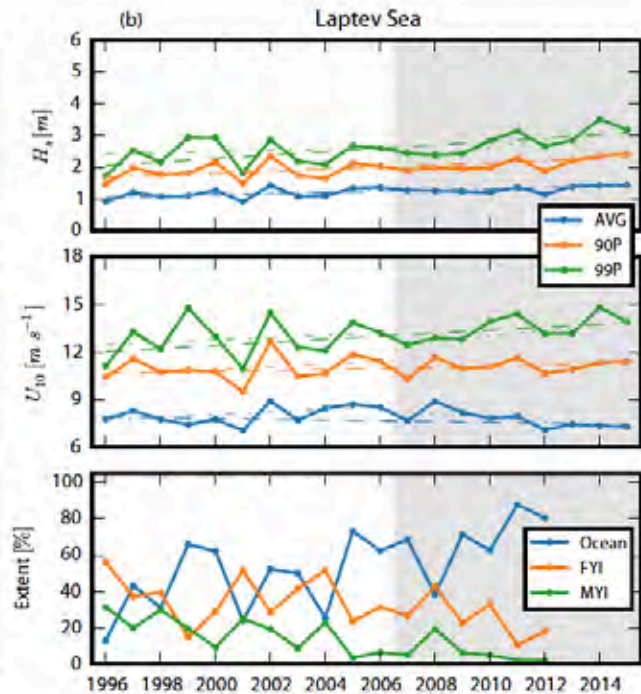
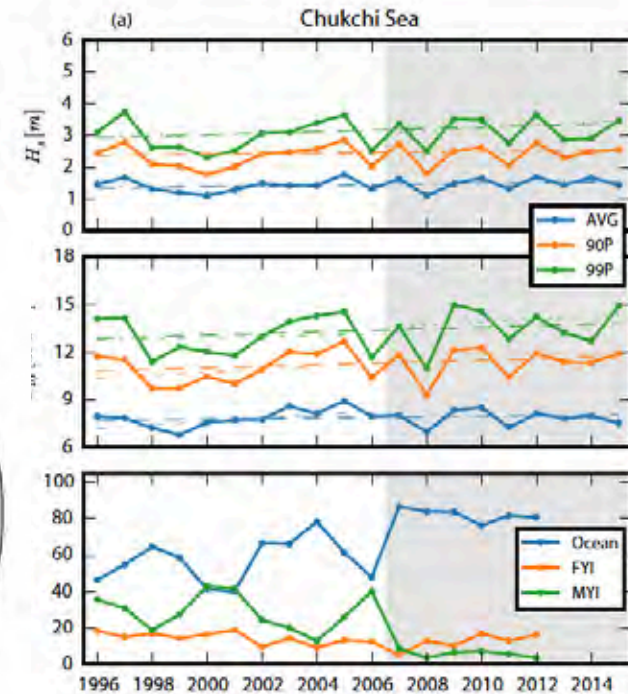
Envi March





Trends before and after 2006





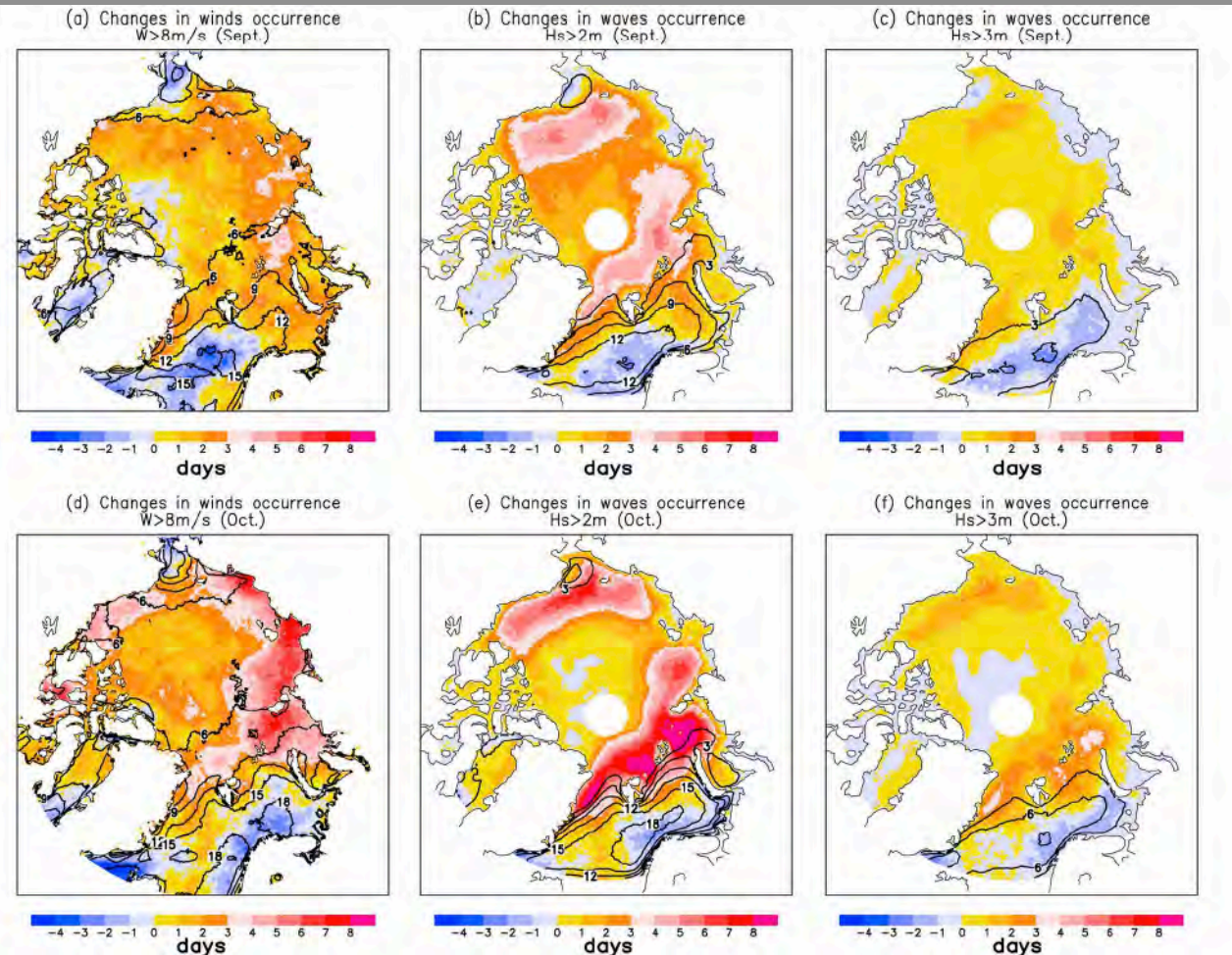


Future Arctic Metocean Modelling

Khon, V.C., I.I. Mokhov, F.A. Pogarskiy, A.V. Babanin, K. Dethloff, A. Rinke, and H. Matthes, 2014: Wave heights in the 21st century Arctic Ocean simulated with a regional climate model. *Geophysical Research Letters*, 41, 2956-2961

Climate/Ice/Wave Modelling

September

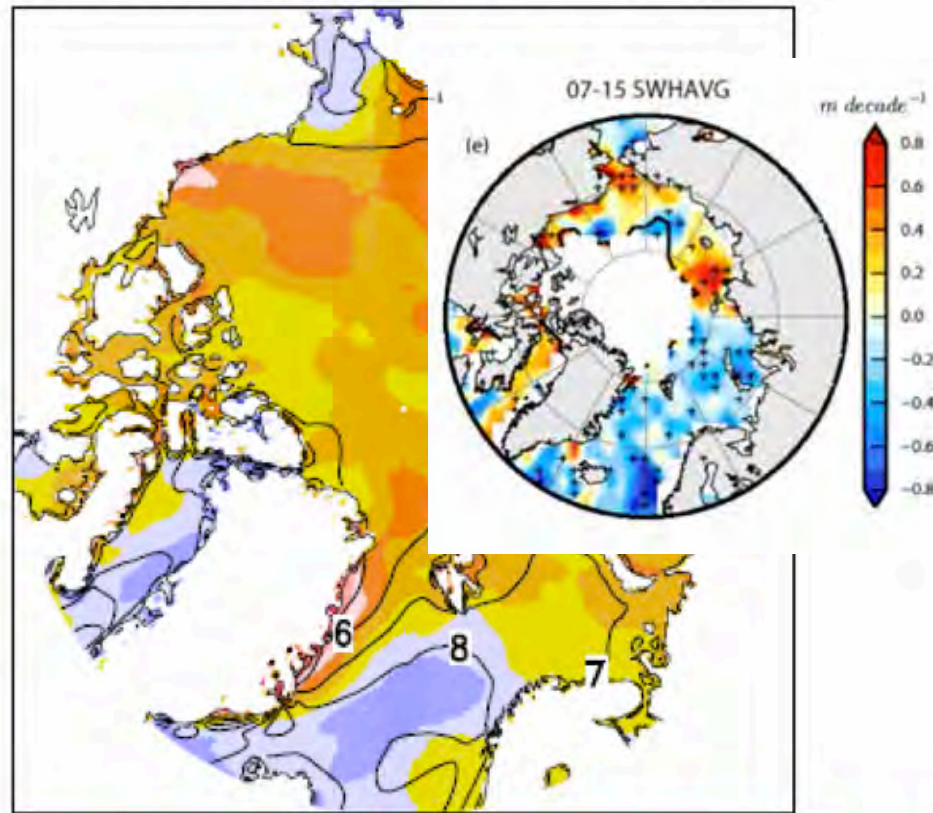


October

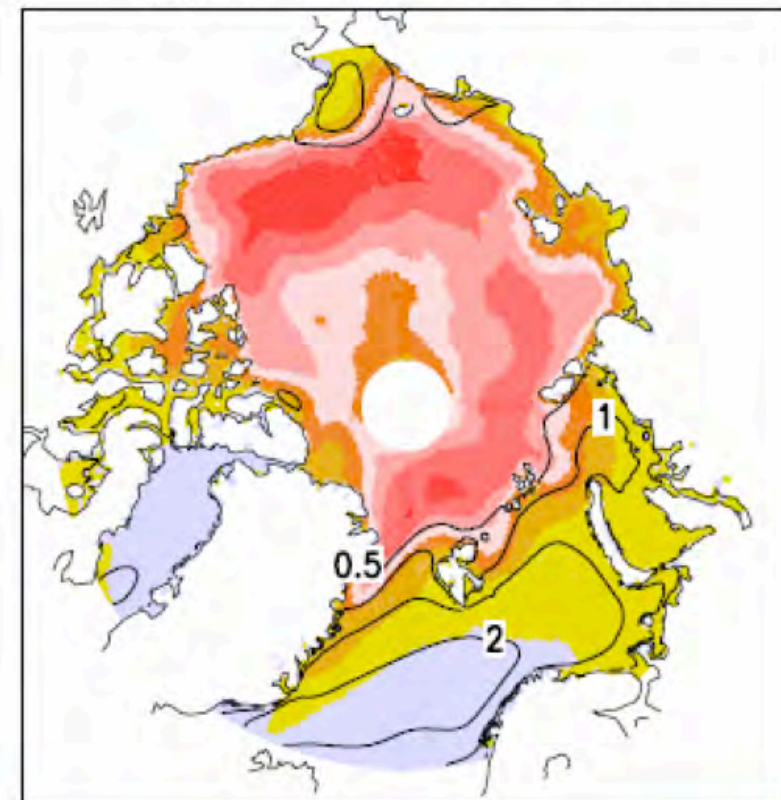
- 2046-2065 relative to 1980-1999
- (left) $U_{10} > 8\text{m/s}$; (middle) $H_s > 2\text{m}$; (right) $H_s > 3\text{m}$

Khon et al., 2014, *GRL*

(c) Rel.changes in mean wind speed



(e) Changes in mean Hs

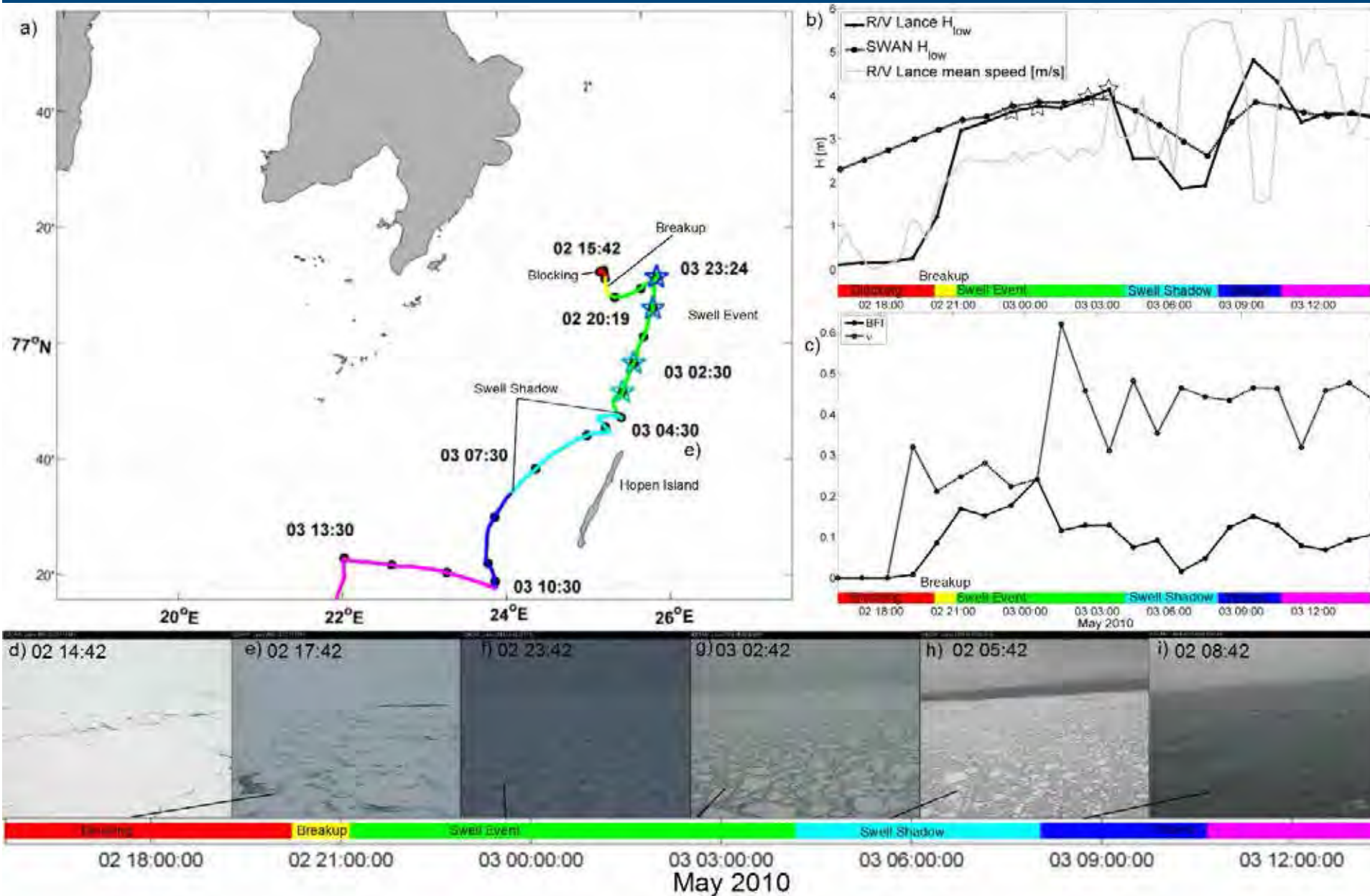


September. Simulated relative changes (%) in mean wind speed at 10 m height (normalized to mean climatological for 1980-1999) and (m) in significant wave height, for the period 2046-2065 with respect to reference period 1980-1999. Contours indicate mean climatological values of for 1980-1999. **Coupled climate, ice and wave models**



Wave Modelling in MIZ

in preparation, *Liu, Q., W.E. Rogers, A.V. Babanin, J.E. Mosig, J. Li, C. Guan*





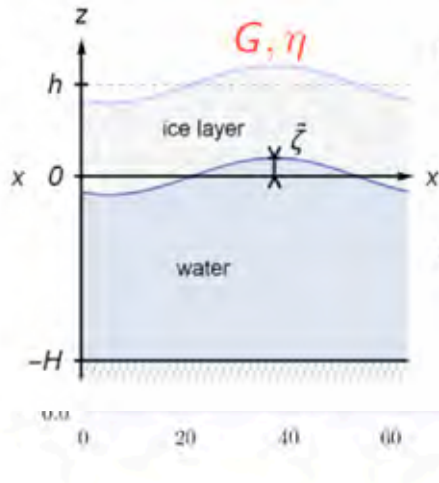
- Dispersion relation of **IC5**

$$Qq\kappa \tanh(\kappa d) - \sigma^2 = 0,$$

$$Q = \frac{G_\eta h_i^3}{6\rho_w g} (1 + \nu)\kappa^4 - \frac{\rho_i h_i \sigma^2}{\rho_w g} + 1,$$

1D Academic test of **IC5** in WW3

The sketch of the viscoelastic models:



Rheological params.:

G : shear modulus (Pa)

η : viscosity ($\text{m}^2 \text{s}^{-1}$)

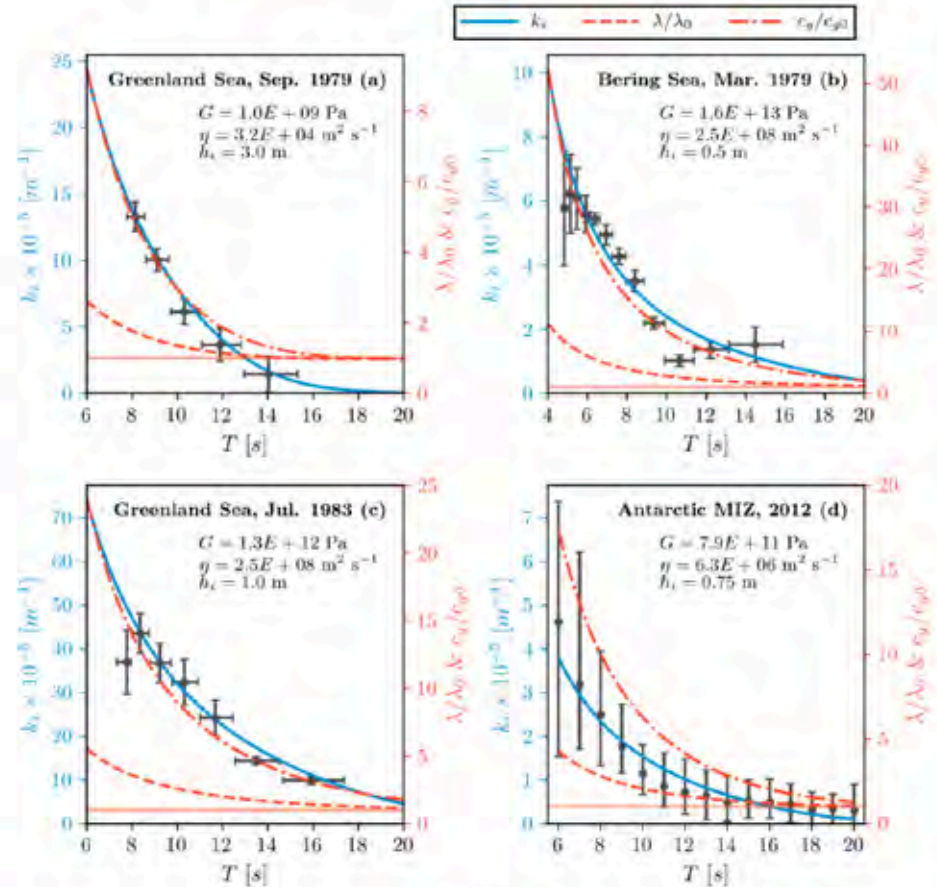
$$G_\eta = G - i\sigma\rho_i\eta$$

Complex wavenumber:

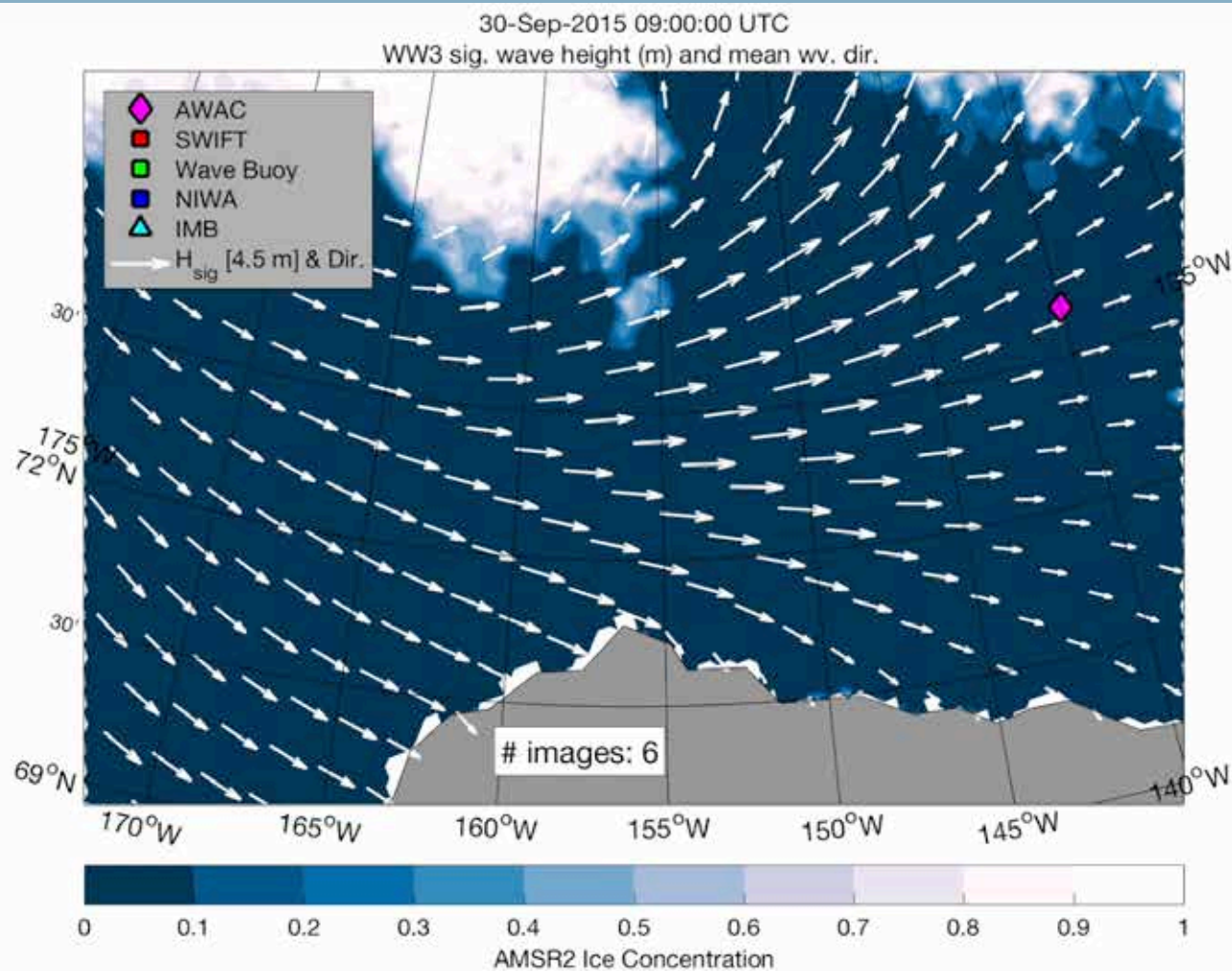
$$\kappa = k_r + ik_i$$

$$k_i = \alpha/2$$

Fit **IC5** to field observations



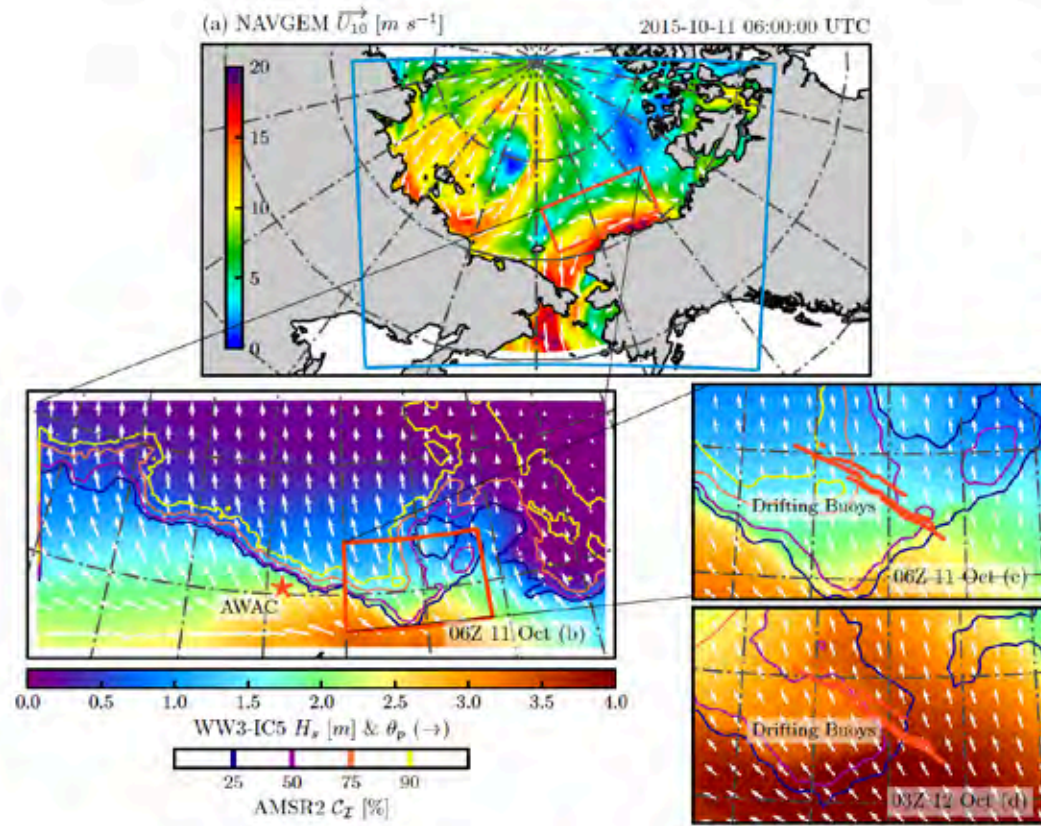
Data from Wadhams et al. (1988) and Meylan et al. (2014)



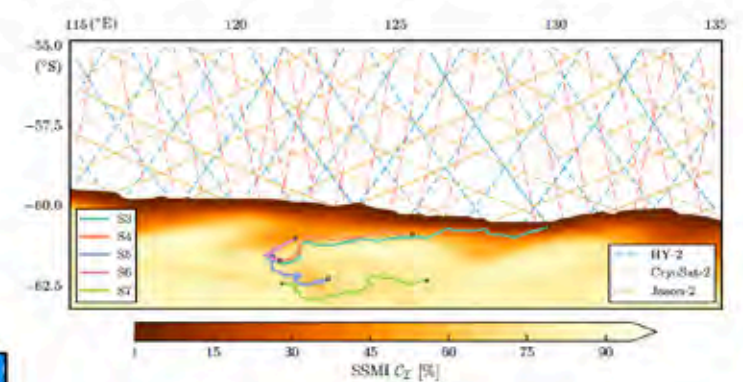
4. Numerical Simulations of Waves in Ice

Two case studies

R/V Sikuliaq Cruise 2015 ($h_i = 0.15$ m)



SIPEX II Voyage 2012 ($h_i = 0.75$ m)



~20-day obs. of waves in ice (Sep/Oct) (Kohout et al. 2014)

- Sikuliaq: two-curvilinear-grid system
- SIPEX: traditional lon-lat grid

Four-day storm event, Oct 2015 (Rogers et al. 2016, Wadhams and Thomson 2015)

Altimeter Data for ONR Sea State DRI Cruise

Swinburne



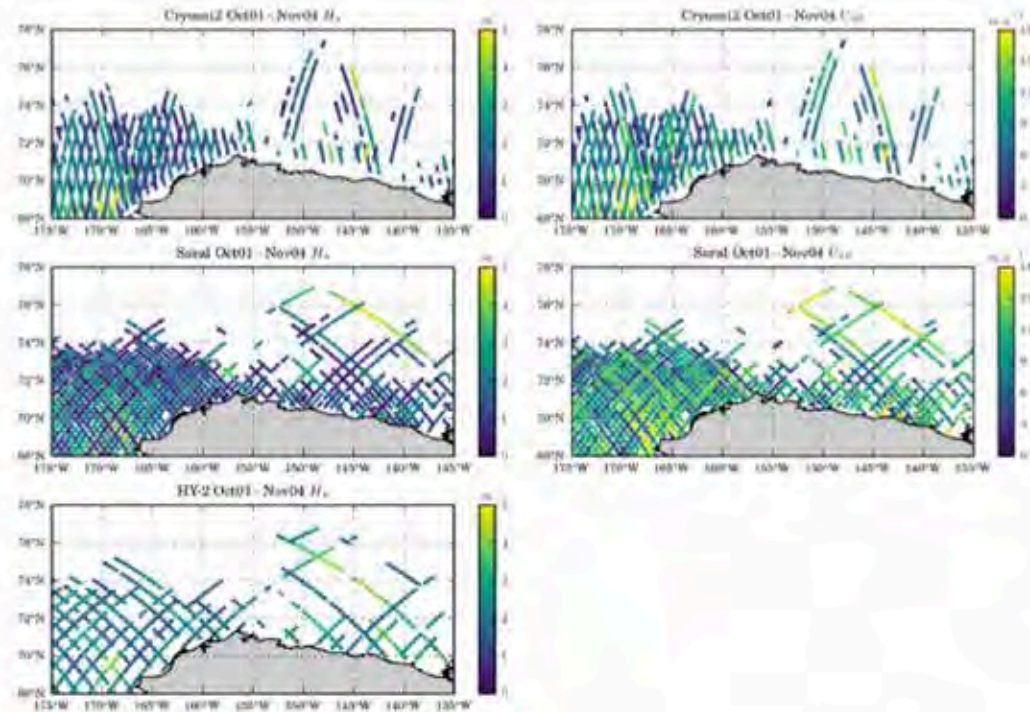
○ Altimeter Data

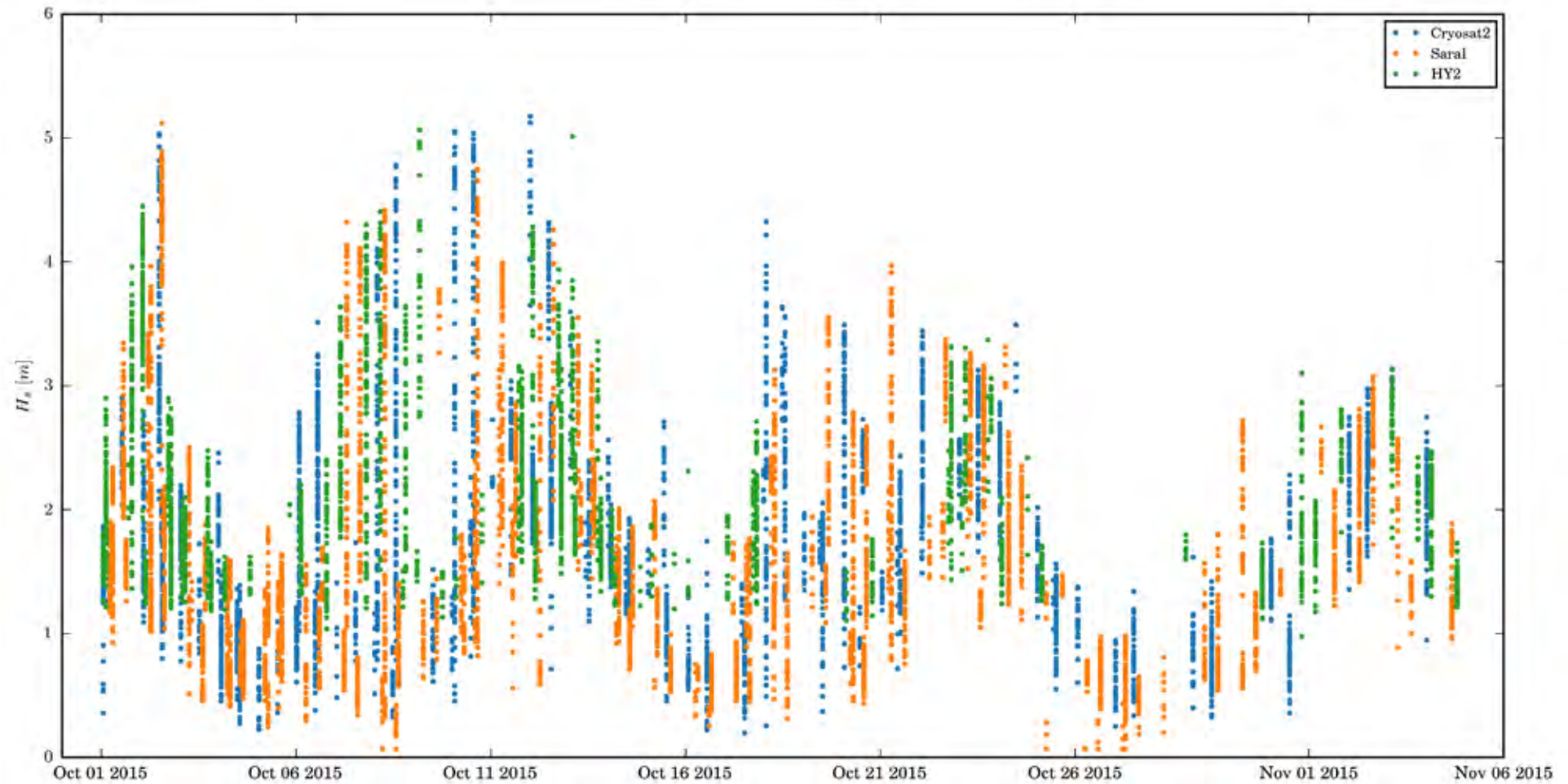
- Cryosat2 wind data were derived from Abdalla (2012) wind model
- HY-2 wind data were excluded because of some issues
- See Zieger et al. (2009) for methodology

altimeter	Band	Data Type	Source	H_s calibration	U_{10} calibration
Cryosat2	Ku	IGDR	NOAA/NESDIS	$H_s^* = \begin{cases} 0.836 \cdot H_s + 0.157 & H_s \leq 1.853m \\ 1.001 \cdot H_s - 0.149 & H_s > 1.853m \end{cases}$	$U_{10}^* = 1.035 \cdot f(\alpha_0 - 0.006) - 0.252$
Saral	Ka	GDR-T	AVISO	$H_s^* = 0.997 \cdot H_s - 0.056$	$U_{10}^* = 1.124 \cdot U_{10} - 0.322$
HY-2	Ku	IGDR	NSOAS	$H_s^* = \begin{cases} 0.977 \cdot H_s + 0.187 & H_s \leq 3.568m \\ 0.013 \cdot H_s^2 + 1.083 \cdot H_s - 0.359 & H_s > 3.568m \end{cases}$	/

○ Data for Cruise

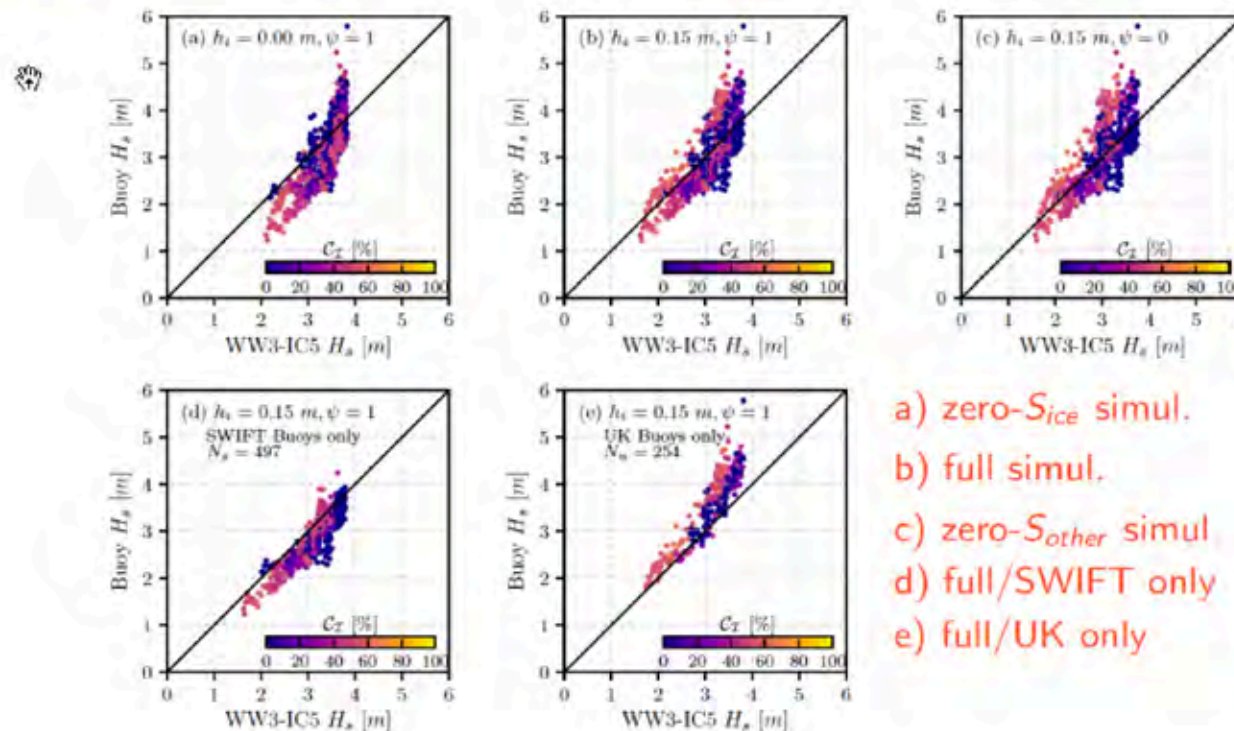
- Lon: 175 W – 135 W
- Lat: 68 N – 78 N
- Period: Oct 1 – Nov 5, 2015
- Cruise was mainly limited in the red rectangle





5. Results & Discussions

5.1 R/V Sikuliaq Cruise 2015



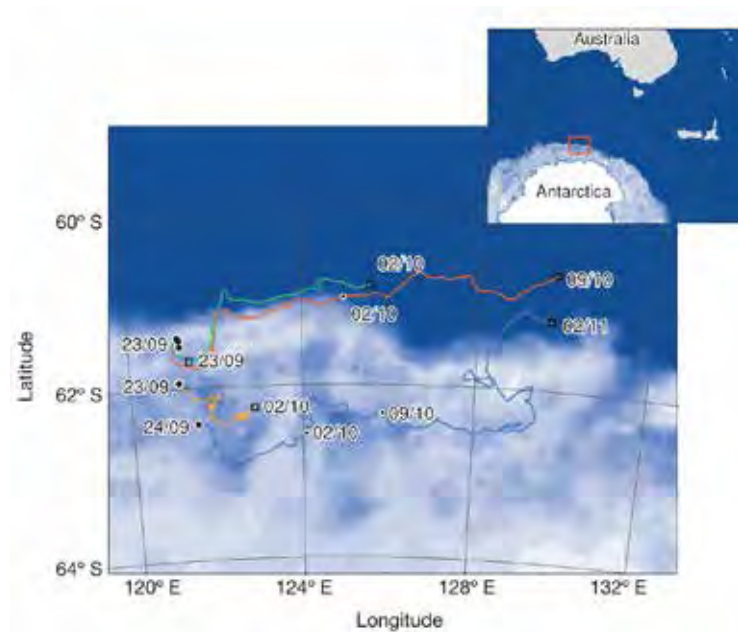
- a) zero- S_{ice} simul.
- b) full simul.
- c) zero- S_{other} simul
- d) full/SWIFT only
- e) full/UK only

Case	ψ	h_i [m]	N	b^\dagger [m]	ε [m]	ρ	SI
R/V Sikuliaq Cruise 2015	1	0.00	751	0.21	0.51	0.82	0.15
$G = 10^7$ Pa $\eta = 4 \times 10^3$ m ² s ⁻¹	—	0.15	—	0.01	0.45	0.79	0.14
	0	—	—	-0.09	0.48	0.76	0.15

[†] bias b , RMSE ε , correlation coefficient ρ and scatter index SI

Work in progress

- Replacing the constant ice thickness with new ice thickness field data from SMOS
- Run another case study



SIPEX II voyage wave data from Kohout et al. (2014)

Dissipation and dispersion

- + visco-elastic
- - turbulent

Ice breakup

Attenuation and dispersion

- mass loading
- floe-floe collision
- rafting
- overwash

Coupled effects

- ice melts (sunshine, wave mixing) , fetch grows
 - ~~ice refreezes (cold air), ice cover grows~~
-



Ice material properties

- viscoelastic
- brittle
- porous
- depends on temperature and salinity
- solid ice
- pancake ice
- frazil ice

Pilot numerical modelling project is under way

Cold room?

crash ice tests





Wave-ice interactions

in preparation, *D.K.K. Sree, D. Wang, S.M. Parra, T. Collins, A.W.K. Law, A.V. Babanin*



Cold room, air/water temp. control, down to -12°C wave, ice and turbulence measurements





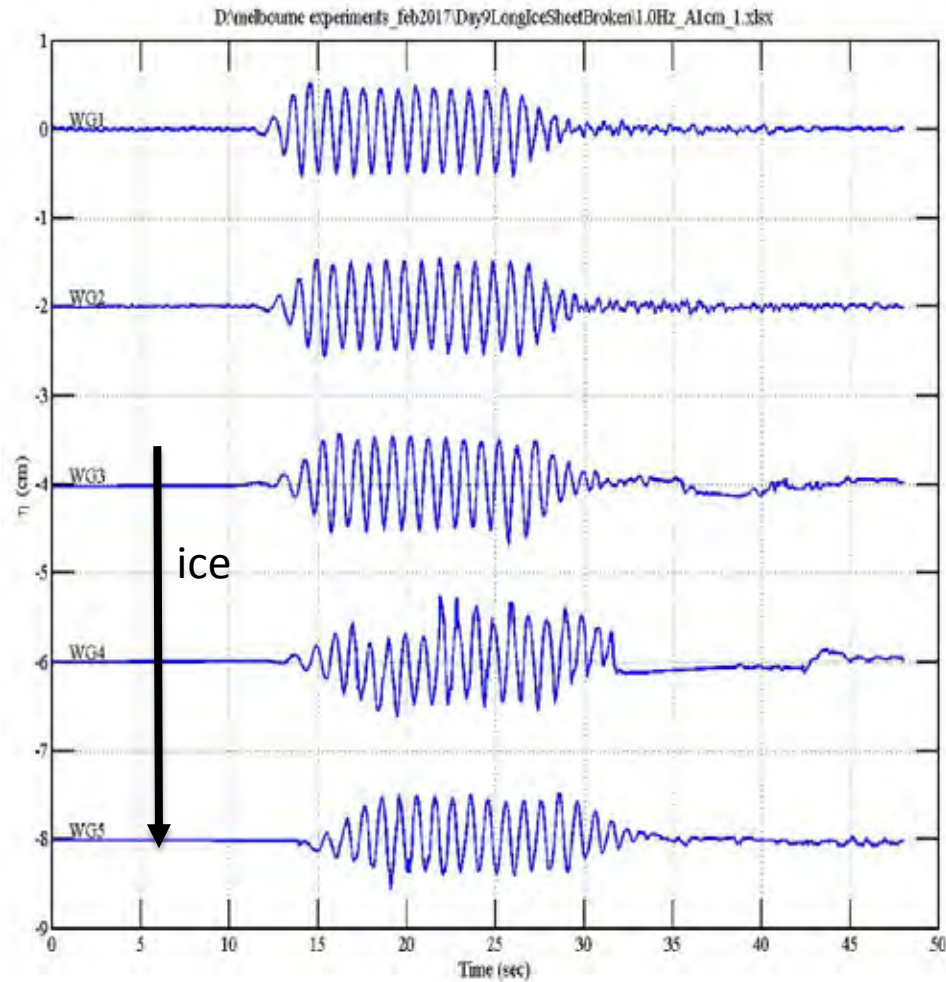
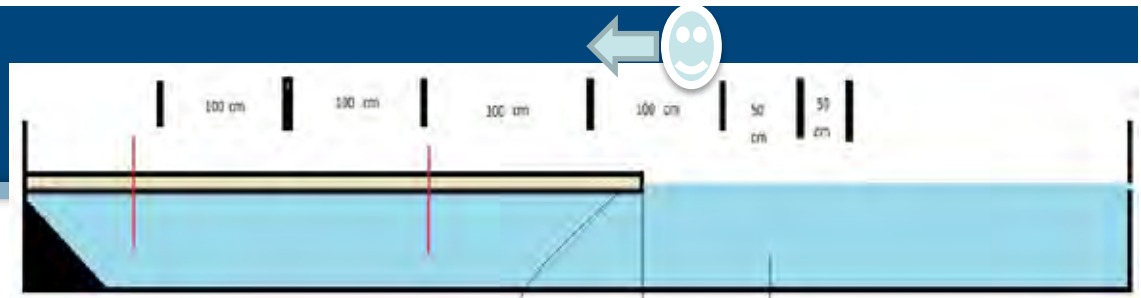
Ice type	# test run	Siwi Day
Thinner Long Ice sheet	34	4
Long Ice sheet broken floes	38	4
Grease Ice 60 %	36	6
Grease Ice 25 %	36	7
Short Ice sheet	40	8
Thicker Long Ice sheet	13	9
Long Ice sheet broken floes	36	9

Long Solid Ice Sheets: Thicker





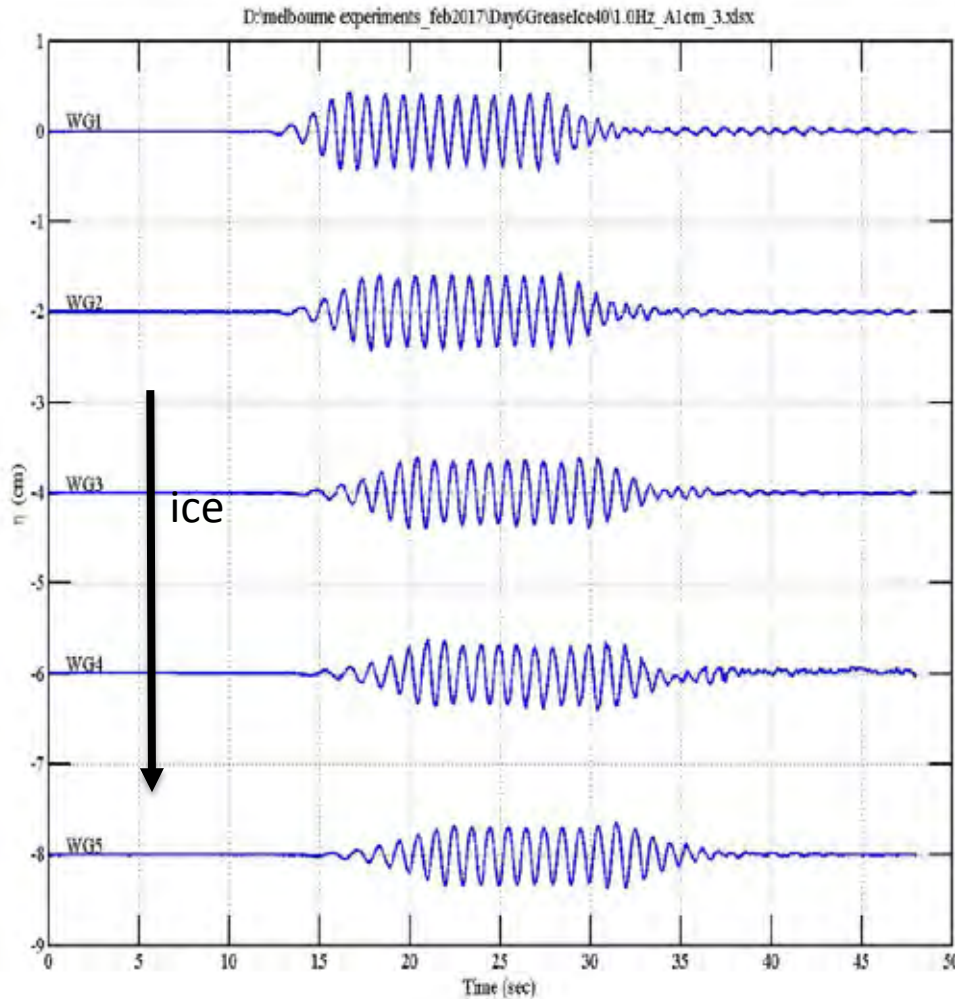
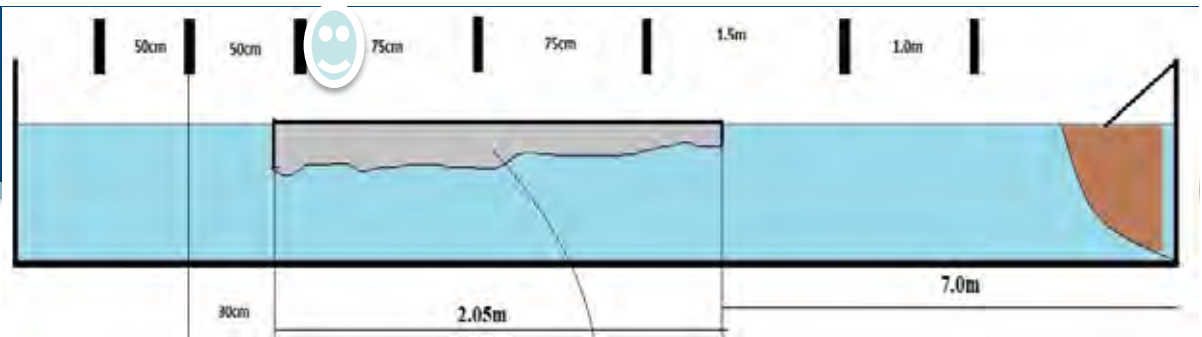
Ice Floes: 0.3-0.7 cm





THE UNIVERSITY OF
MELBOURNE

Grease Ice: 60% concentration

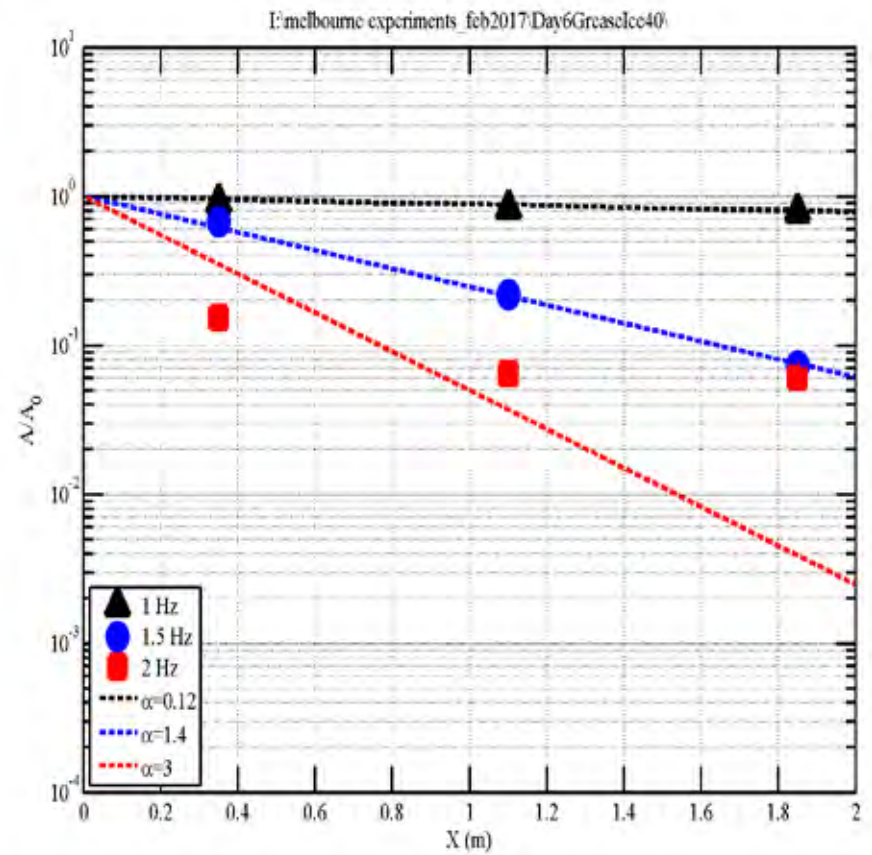
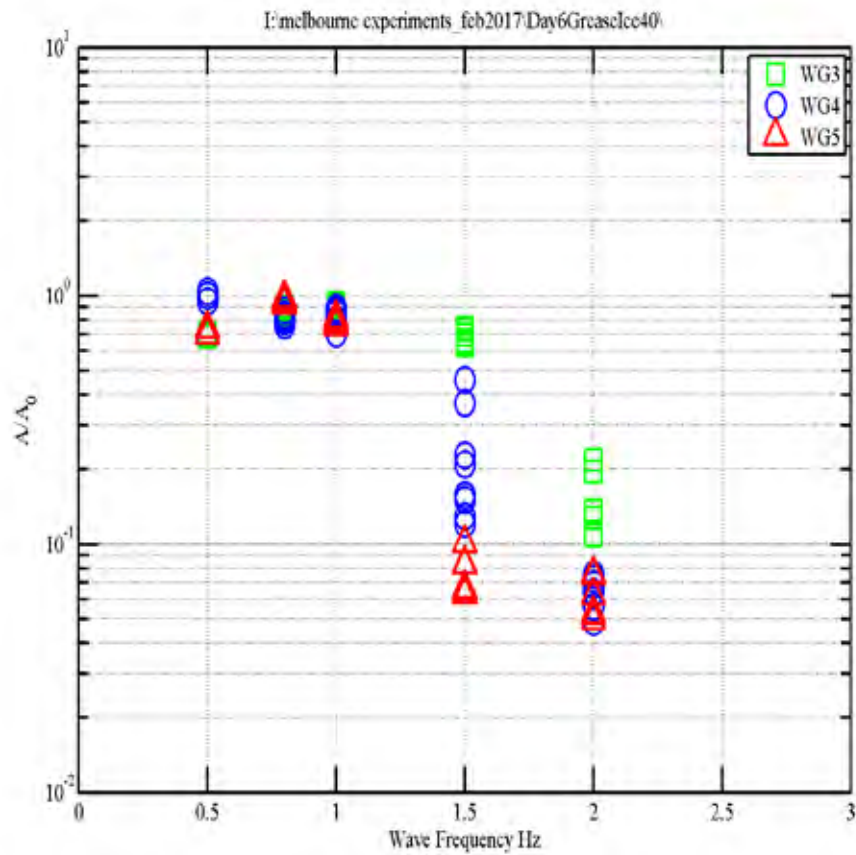
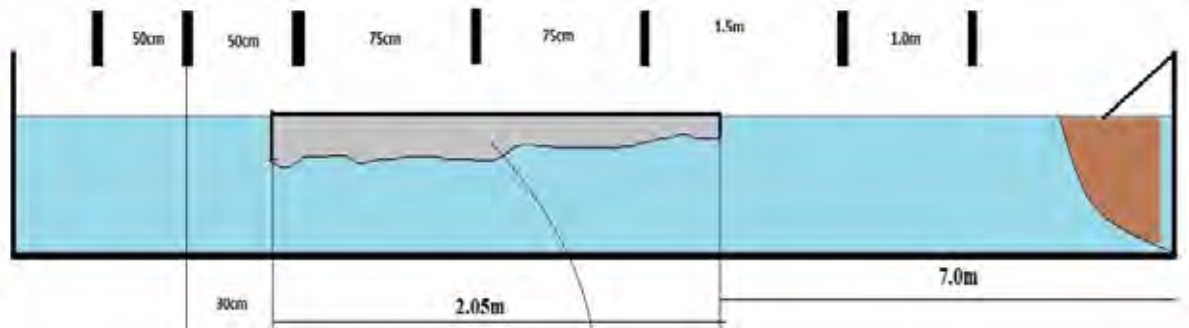


Video during grease making



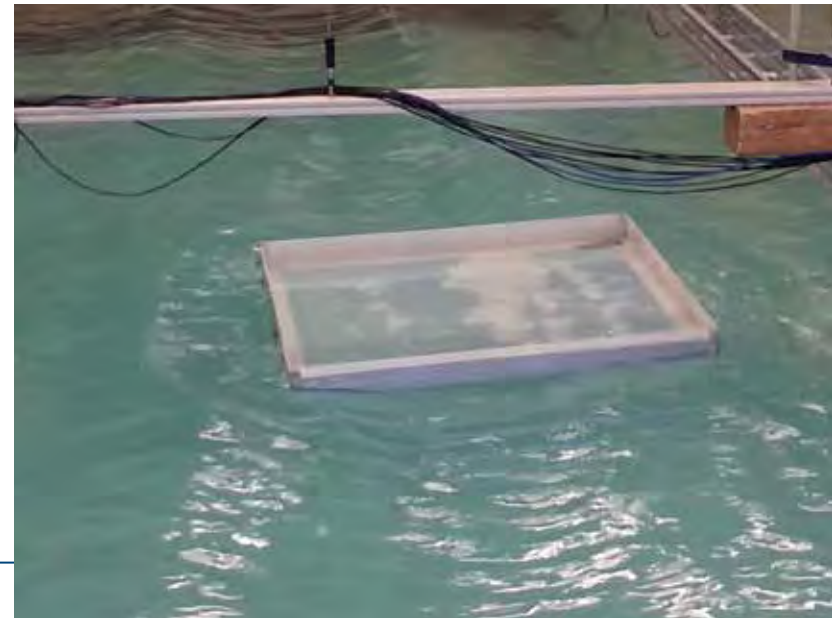
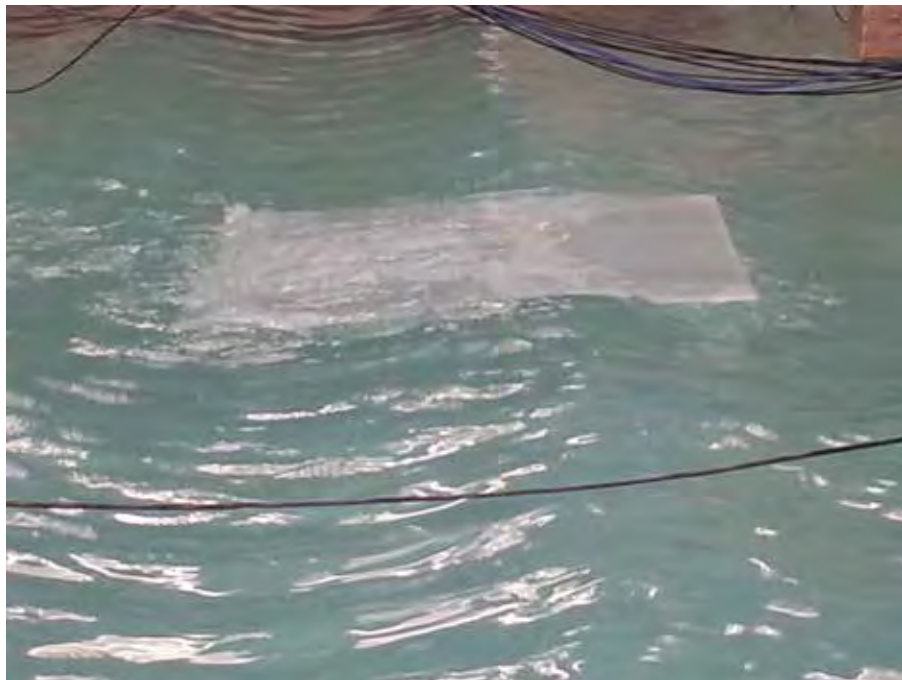
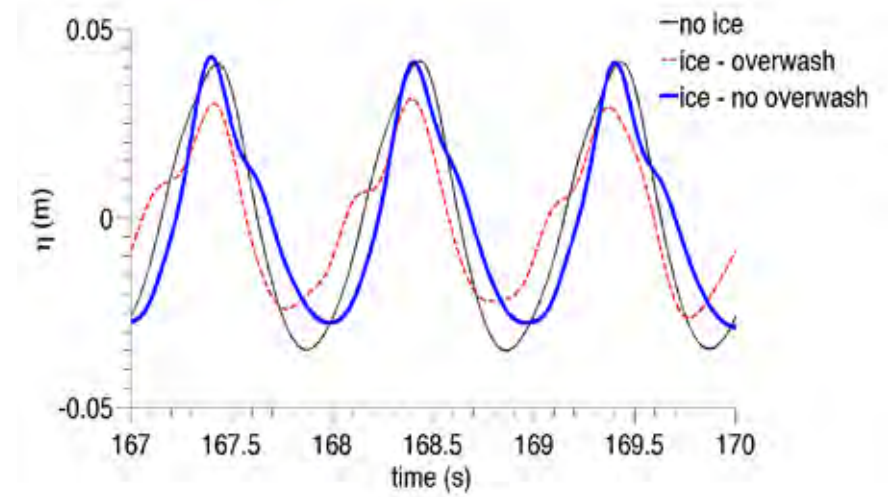


Grease Ice: 60% concentration





Lab Experiments, Uni Plymouth





Wave-induced mixing

in preparation, *S. Thomas, K. Walsh, L. Stoney, A.V. Babanin*

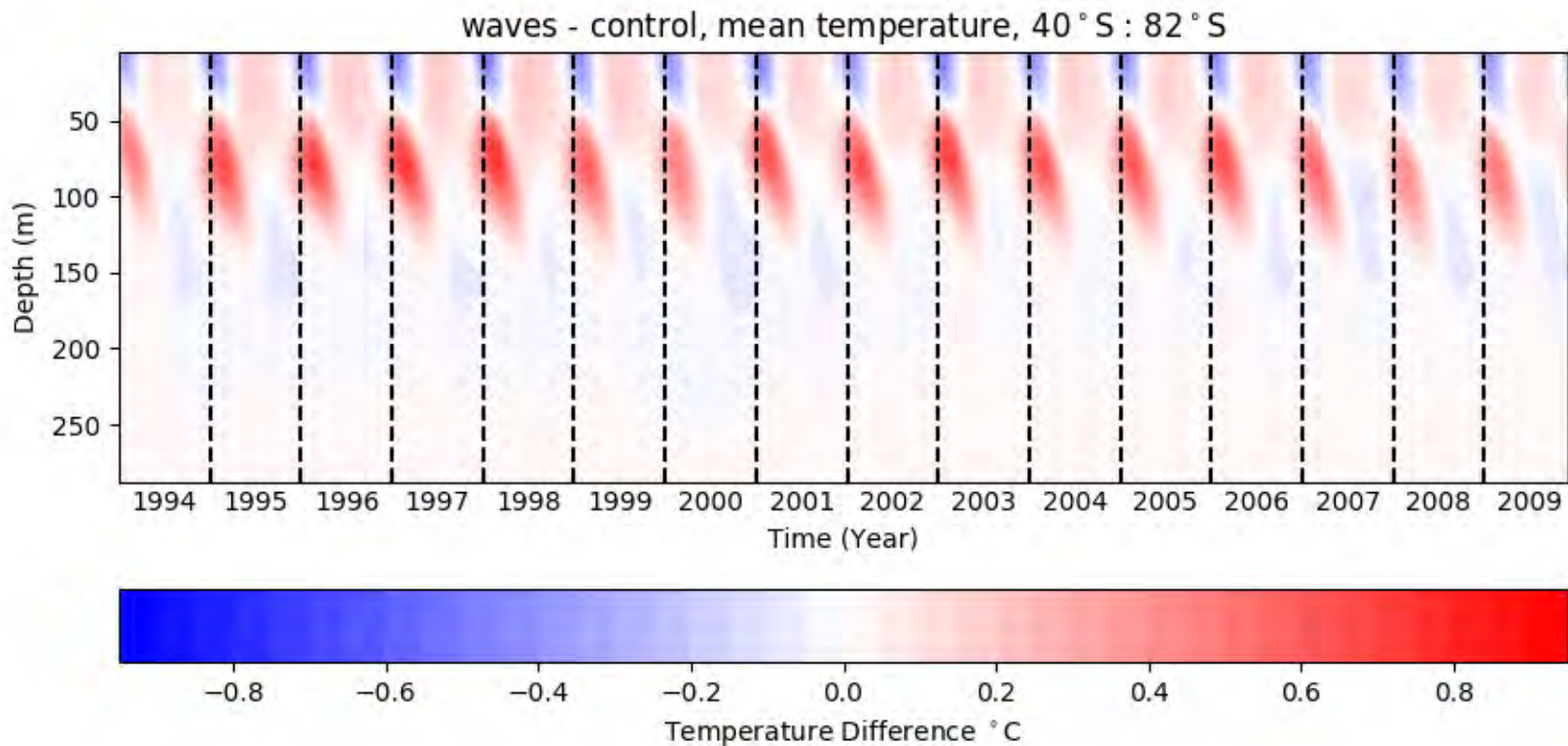
- Wave-induced mixing (MOM5)
- One-way coupling with WW3

In the figures (subsequent slides):

- the anomalies are calculated by taking the difference between the simulation with waves and the simulation without waves
 - the seasonal values come from a 10 year mean
-



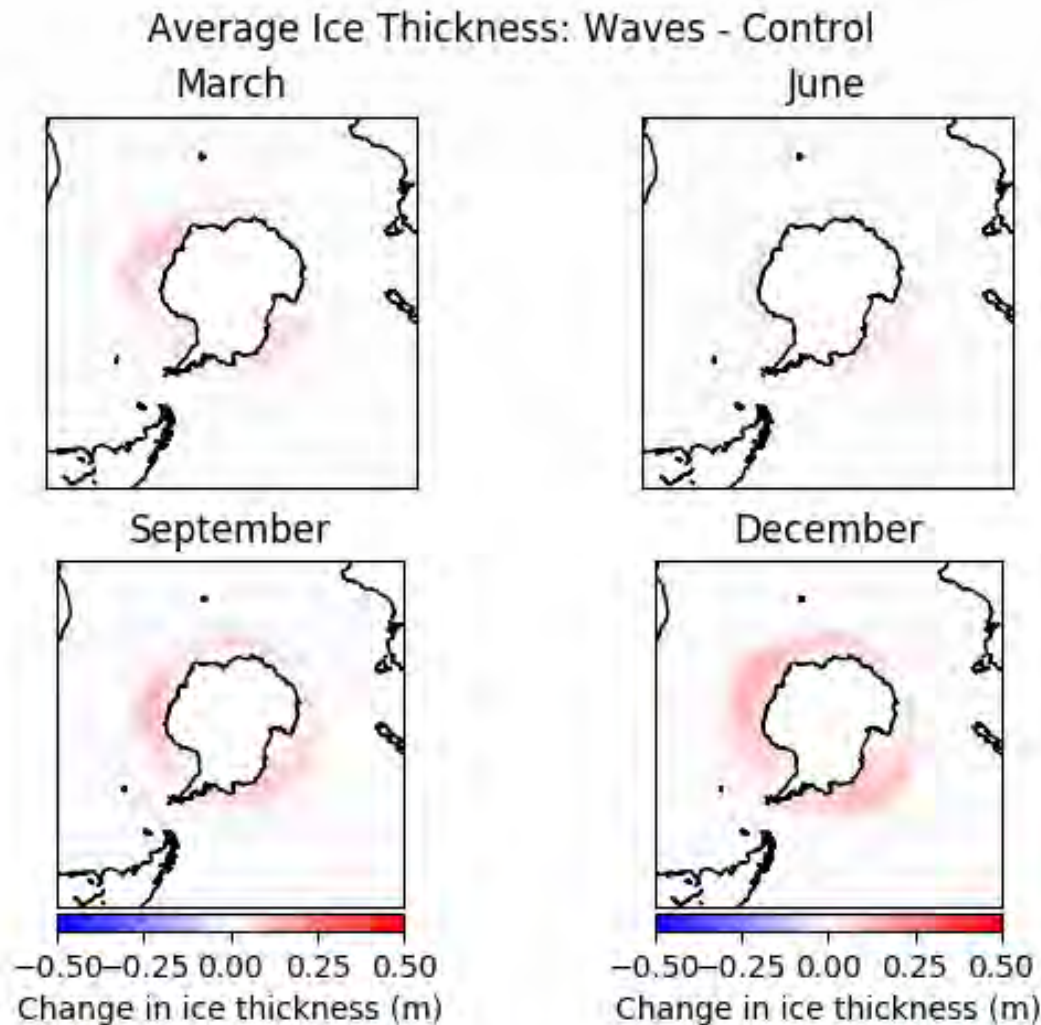
Temperature difference between ocean models with and without the extra wave-mixing term (wave and control, respectively).



In the Southern Ocean an increase in wave mixing captures more heat and transports it into deeper waters over the (southern) summer. While producing a net increase in ocean temperature this results in the waters surface being colder during the summer.



T
N



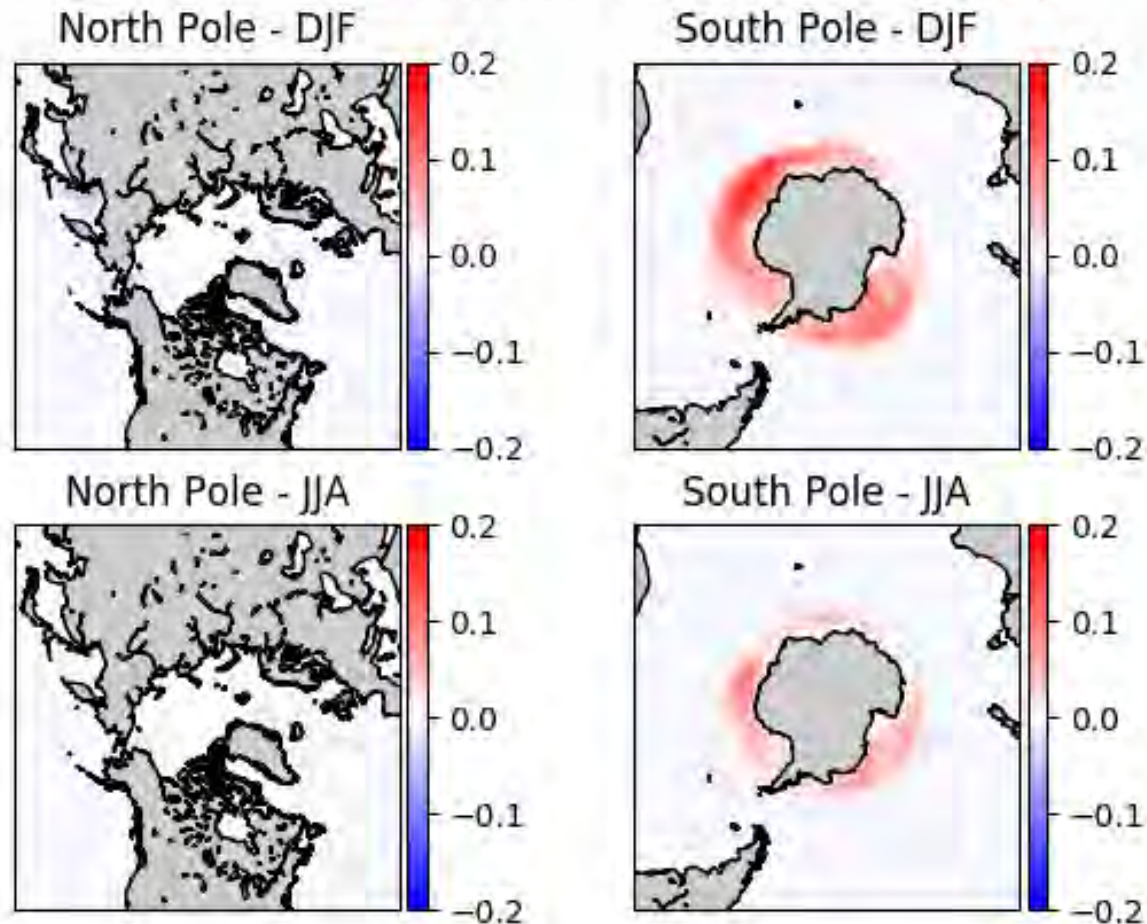
Difference in ice thickness between ocean models with and without the extra wave-mixing term (wave and control, respectively).

The decrease in surface temperature despite the net increase in ocean heat content causes a reduction in the amount of ice melt during the summer.

This results in a thicker Antarctic sea sheet, particularly in December (summer).



Change in ice thickness from increased wave mixing (m)



Difference in ice thickness between ocean models with and without the extra wave-mixing term (wave and control, respectively).

The effect of wave mixing on surface temperatures and thus ice thickness is far less clear in the Arctic with nearby land masses (North America, Russia, etc.) drastically reducing the areas the waves and ice are interacting.



Field observations, Arctic and Antarctica



Hindcast Experiment of waves in ice (wave array #3)



THE ARCTIC OCEAN CRUISE
OF R/V SIKULIAQ 2015

Thomson, J., V. Squire, S. Ackley, E. Rogers, A. Babanin, P. Guest, T. Maksym, P. Wadhams, S. Stammerjohn, C. Fairall, O. Persson, M. Doble, H. Graber, H. Shen, J. Gemmrich, S. Lehner, B. Holt, T. Williams, M. Meylan, and J. Bidlot, 2013: Sea State and Boundary Layer Physics of the Emerging Arctic Ocean. *Science Plan*.





Jan-March
2017

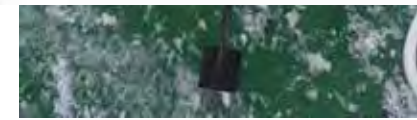
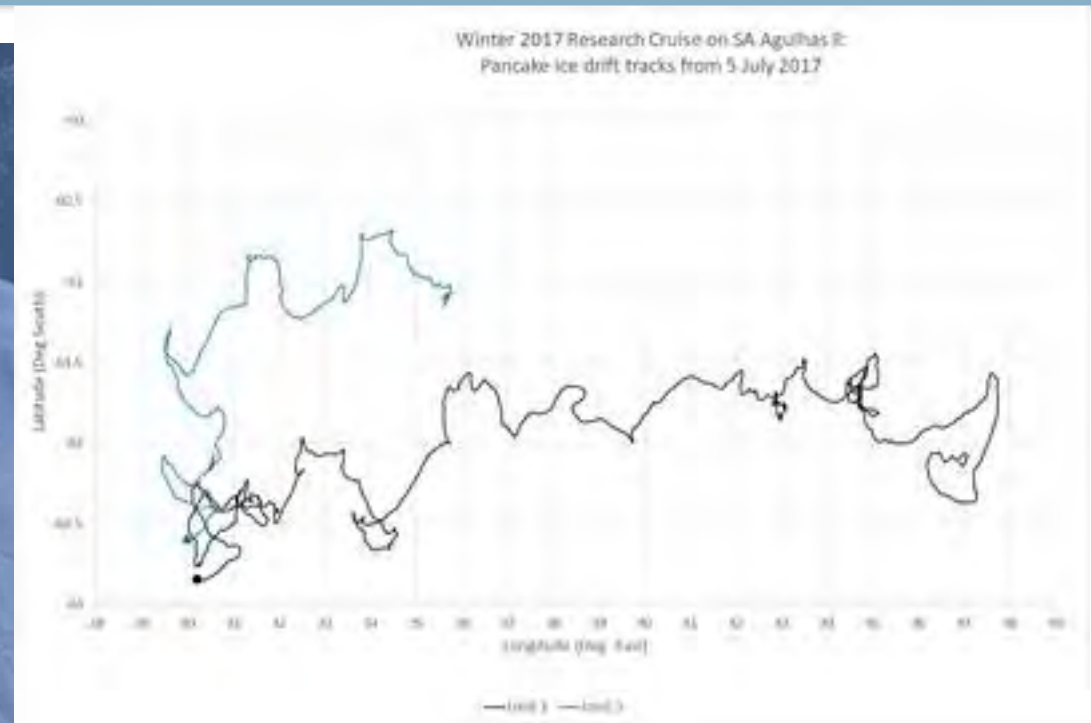
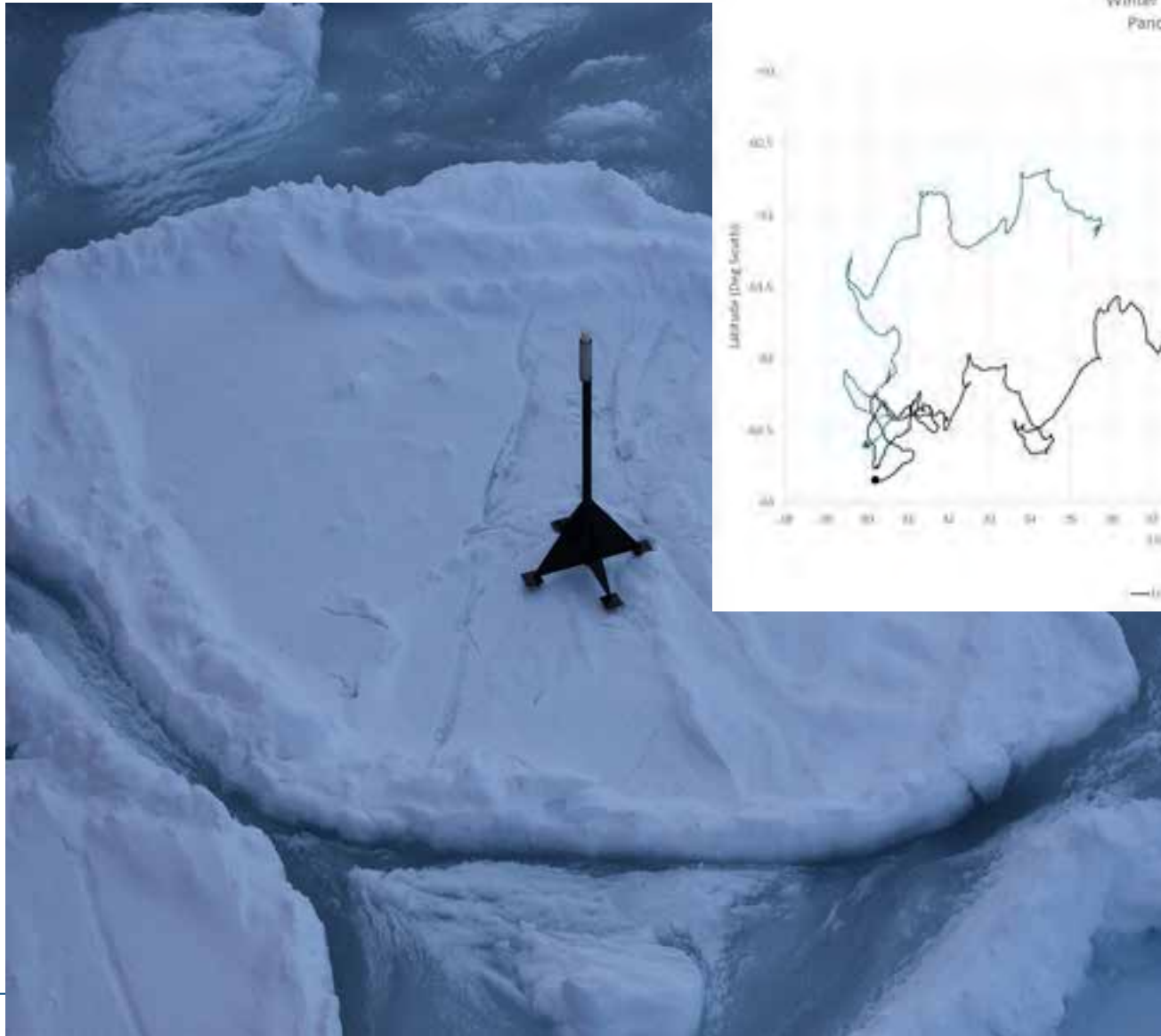
Antarctic circumnavigation expedition Indicative Travel Plan



- WAMOS: waves, currents, ice?
- Satellite observations: ice
- WW3 modelling

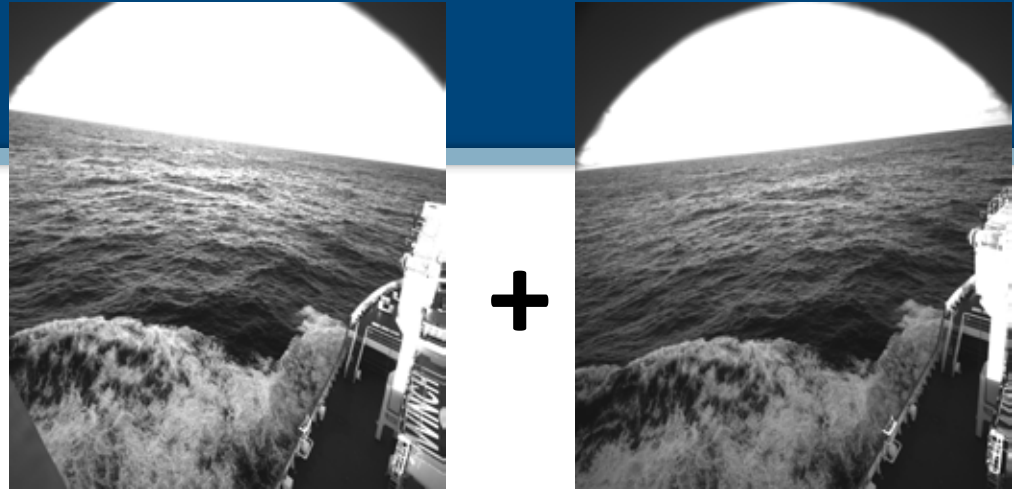


Ice dynamics from GPS trackers



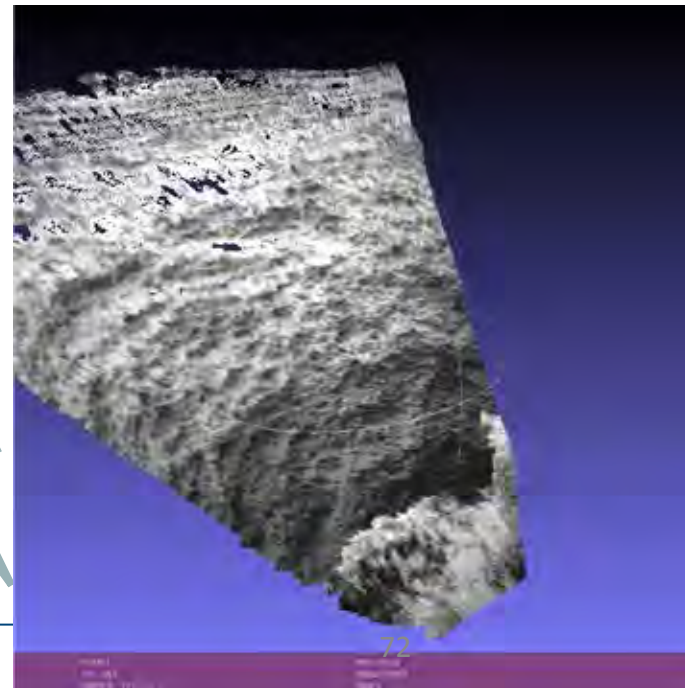


Two
synchronized
cameras



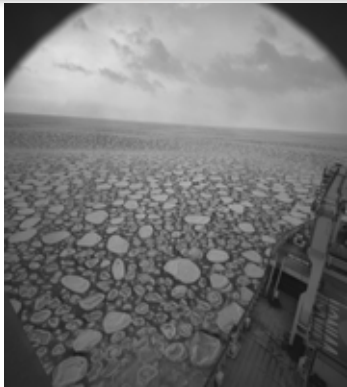
one
IMU

Ocean surface &
Average parameters: wave height,
wavelength, wave direction

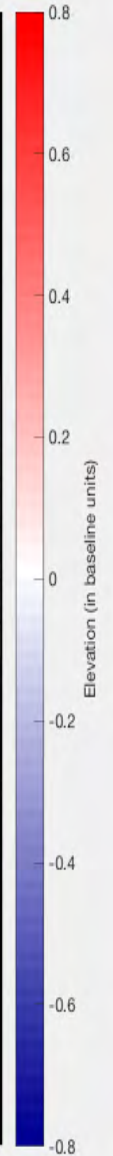
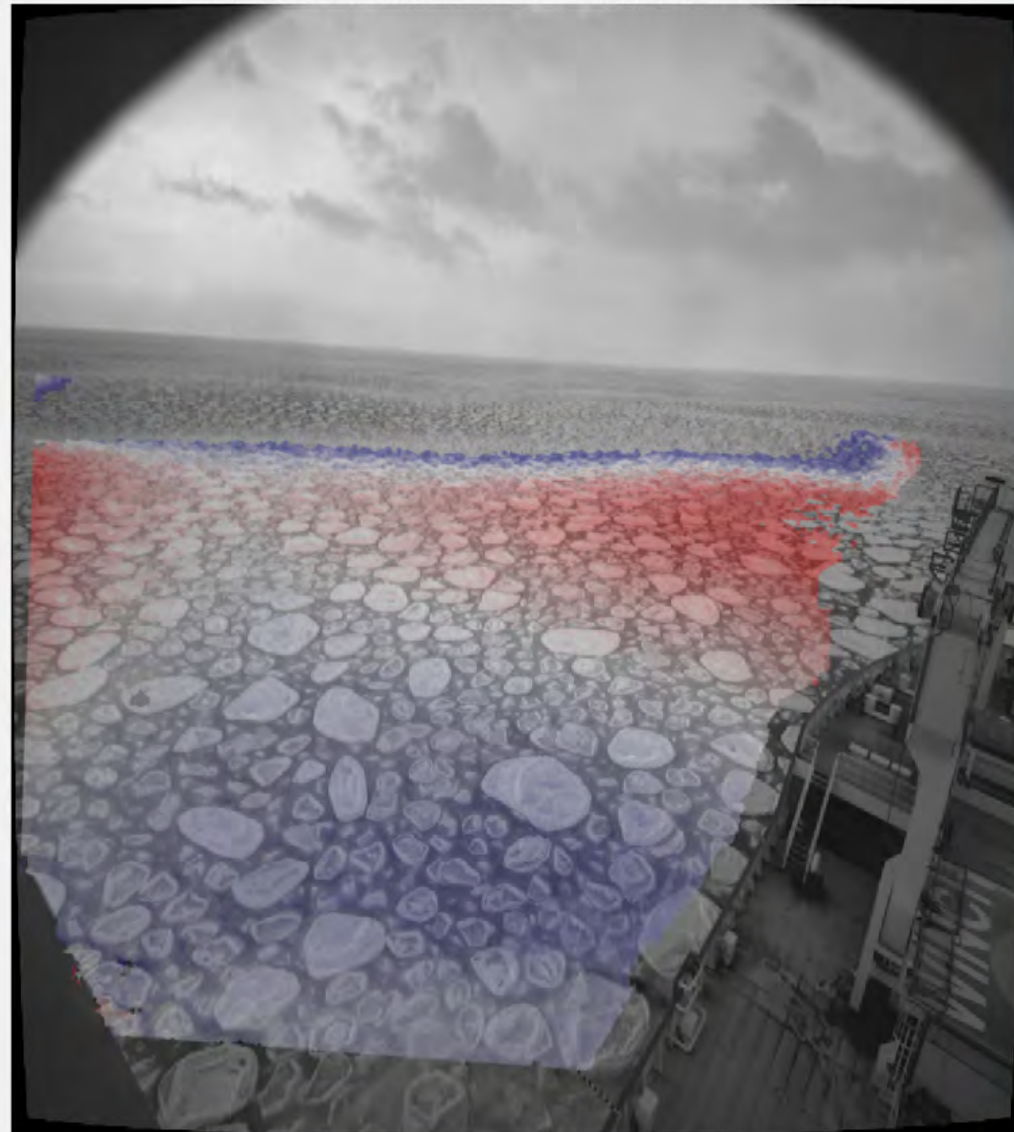




Waves-in-ice from stereo cameras

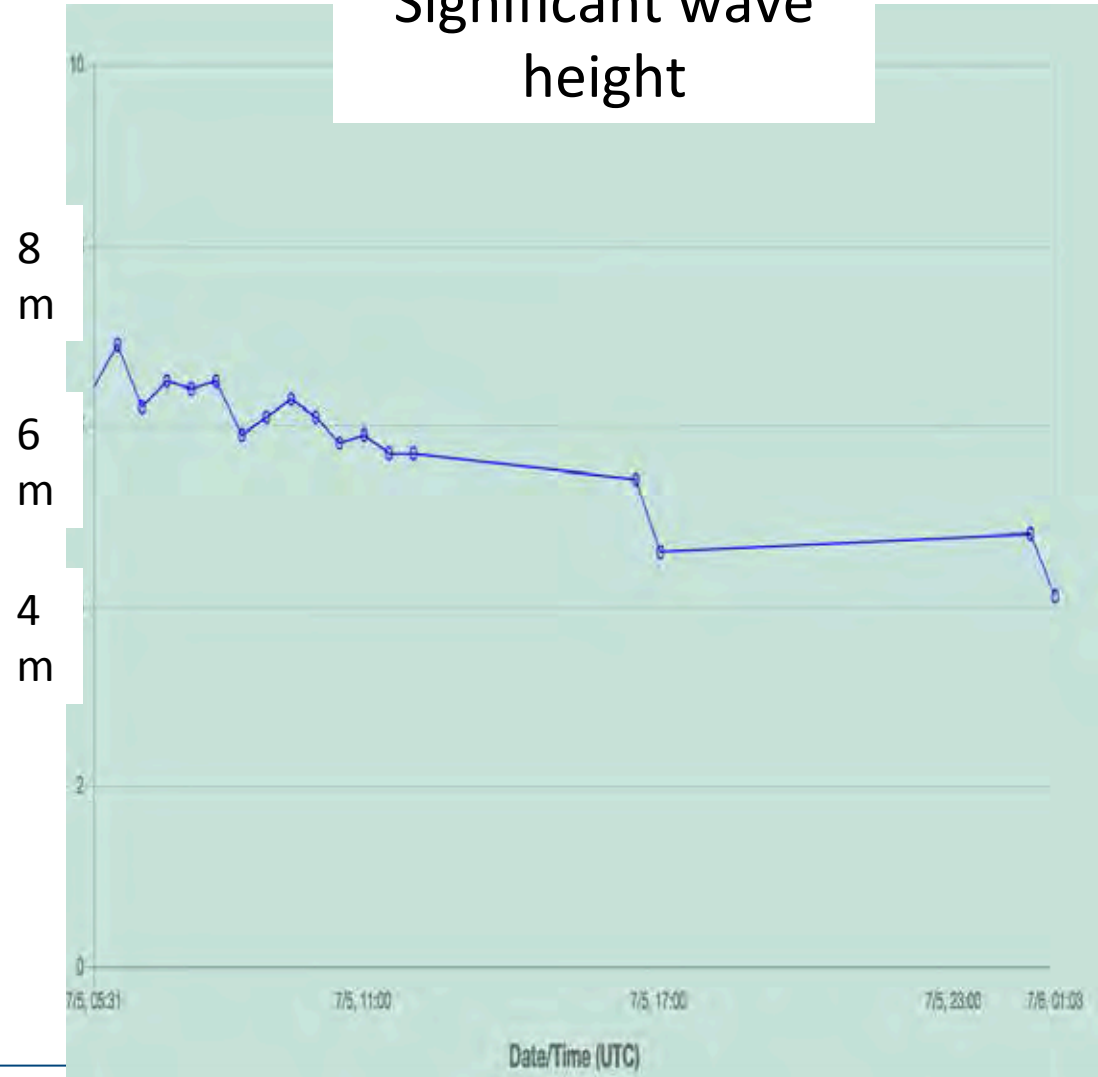


Frame 000000 - 1528112 points - TEST - <http://www.dais.unive.it/wass>





Significant wave height





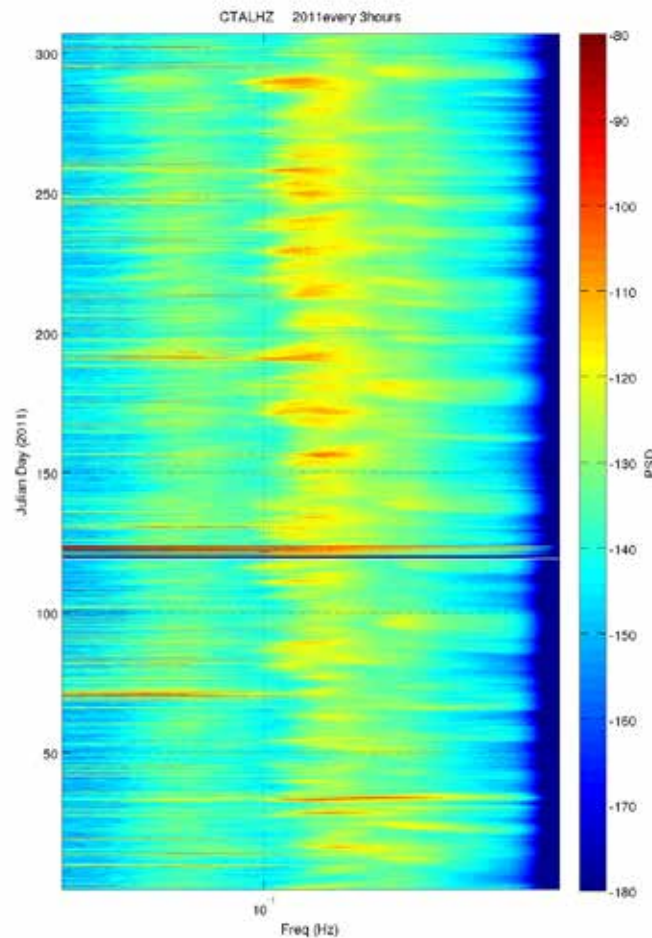
- Metocean climate experiences rapid changes at high latitudes
 - Trends are different between the Arctic and Antarctica
 - Trends are different between different regions of the Arctic
 - In the Arctic, change of the regime occurred around 2006
 - Physics behind Metocean drivers is very uncertain
-
- Wave forecast needs a lot of effort



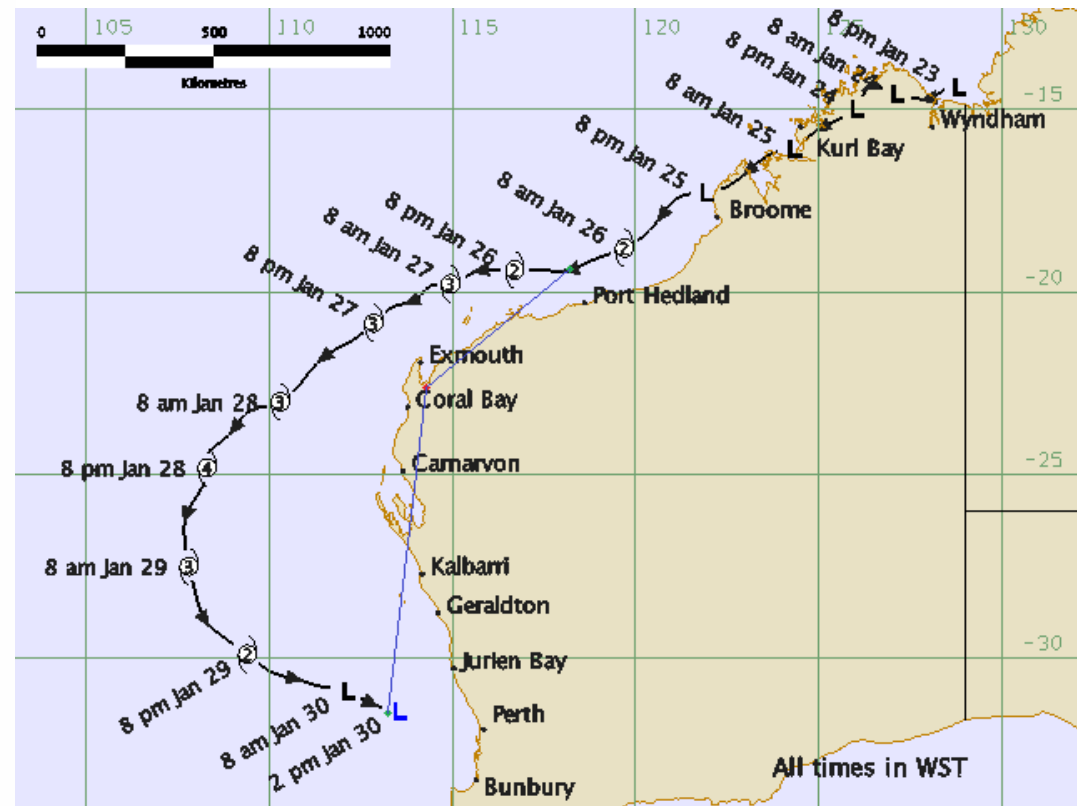
pilot projects



East Coast, 2010

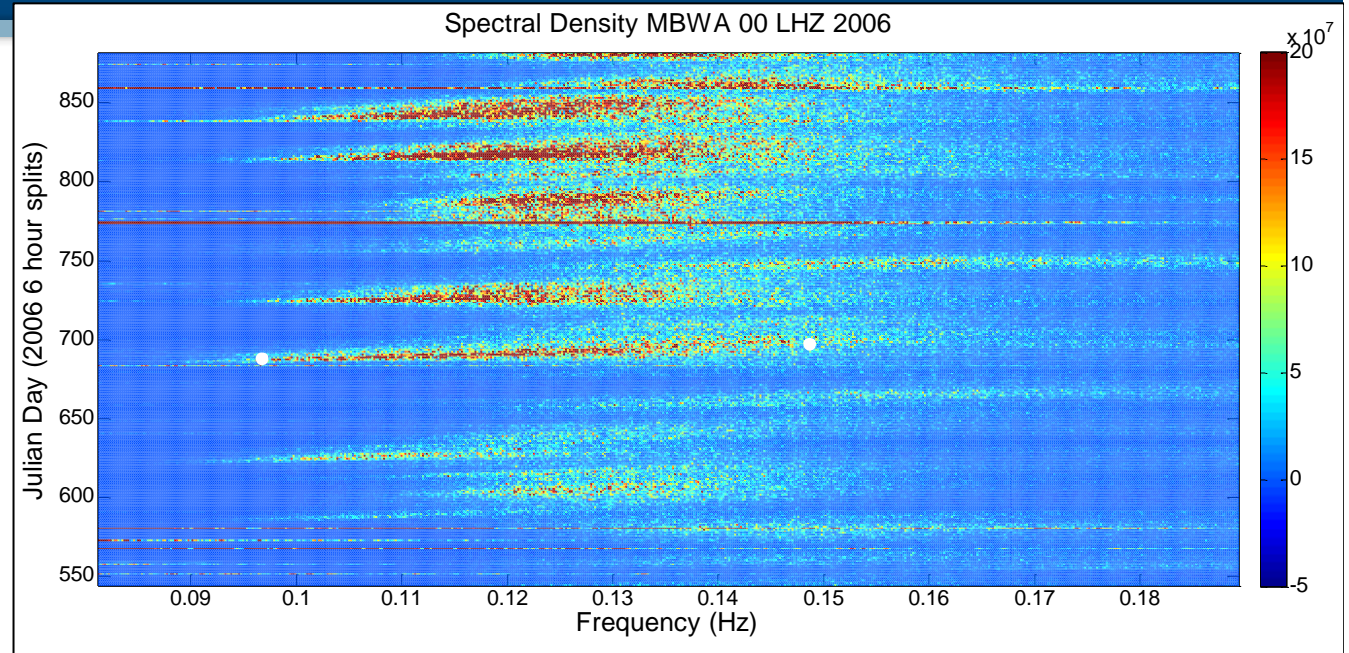
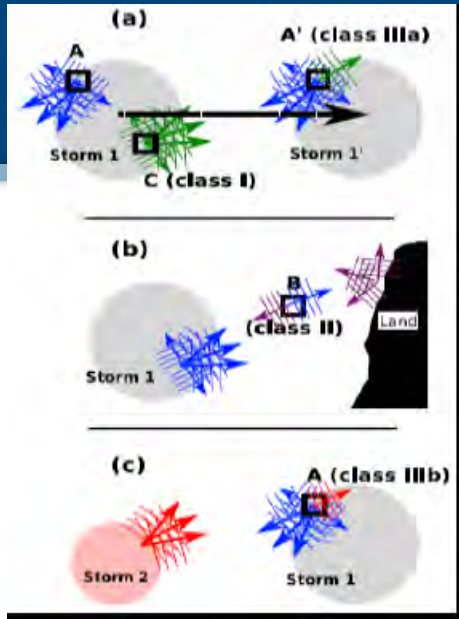


West Coast, Cyclone Bianca

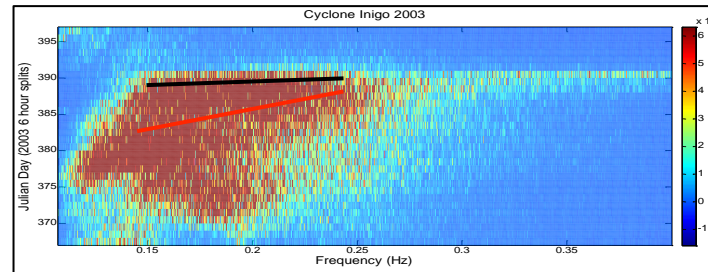
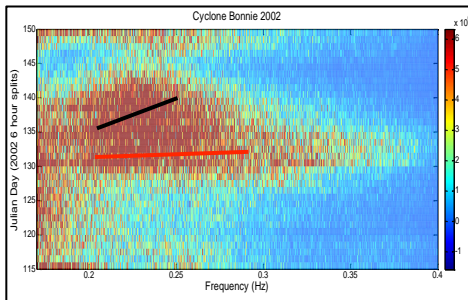


with seismic records being taken since 19th century, this is a possibility to study the wave climate of the past, based on measurements

Tropical Cyclones, NE Indian Ocean



Distance to the cyclone measured by the frequency slope



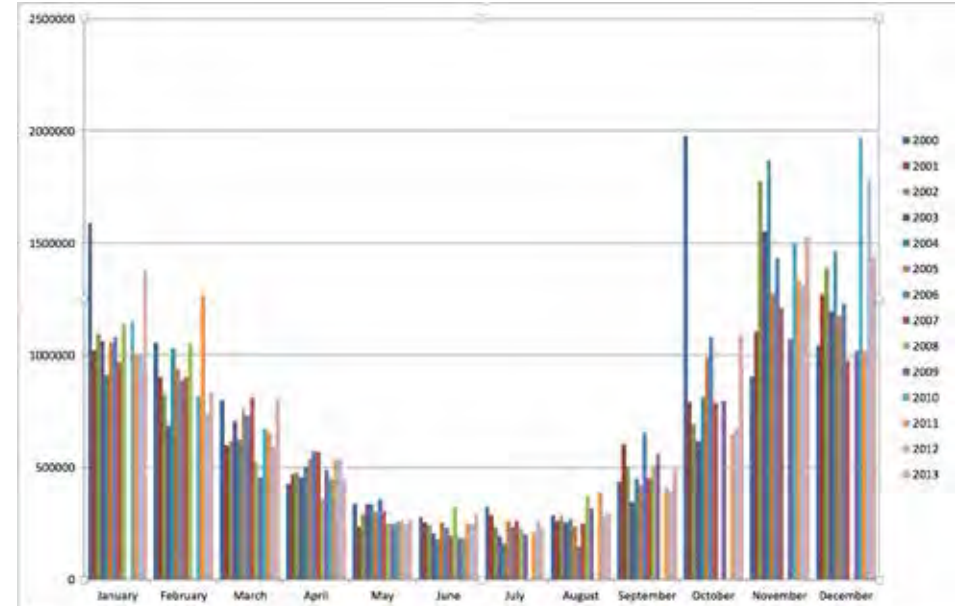
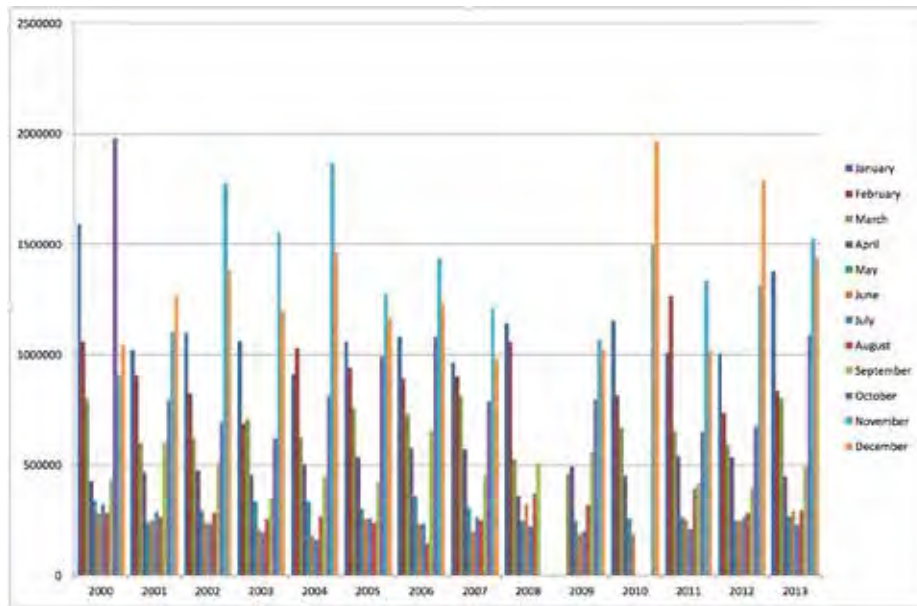
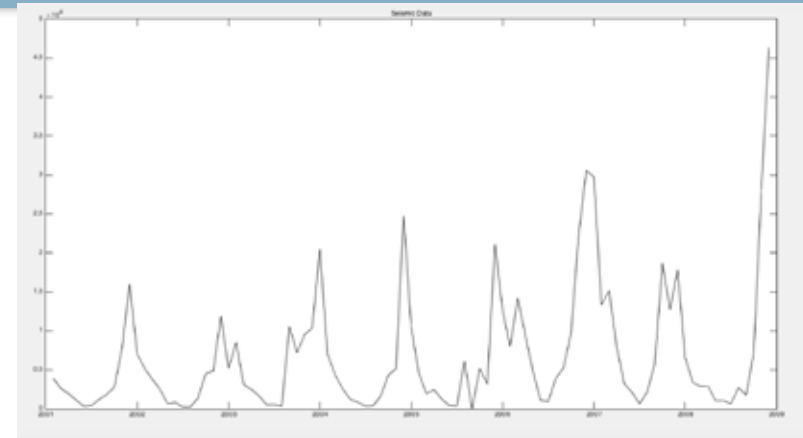
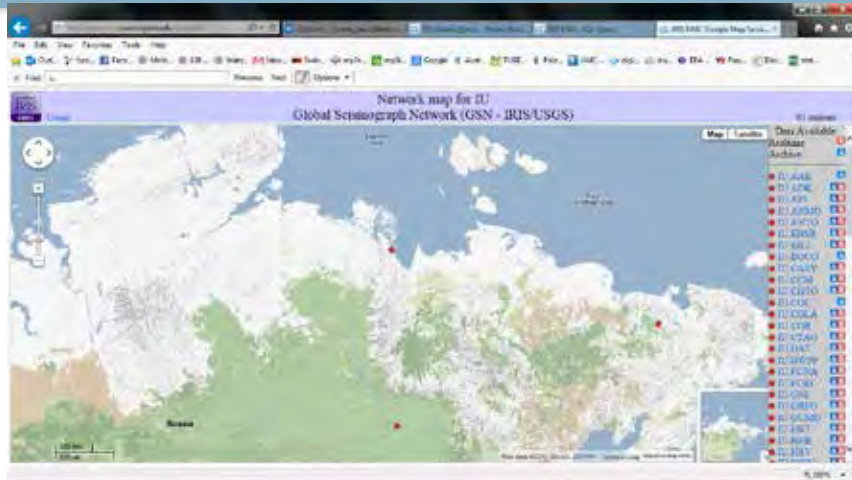
TC Indigo trending towards



TC Bonnie moving away



Waves and Ice, Arctic Ocean



Tiksi records of waves in the Pacific



- Metocean research at the University of Melbourne is outlined
 - Advanced phase-resolving and phase-average models are described
 - Long-term, global and regional wind-wave-ice trends are demonstrated
 - Role of the waves as a link between the ocean and atmosphere is discussed
 - Links of ocean waves to seismic geophysical applications established
-



THE UNIVERSITY OF
MELBOURNE



Waves, measurements

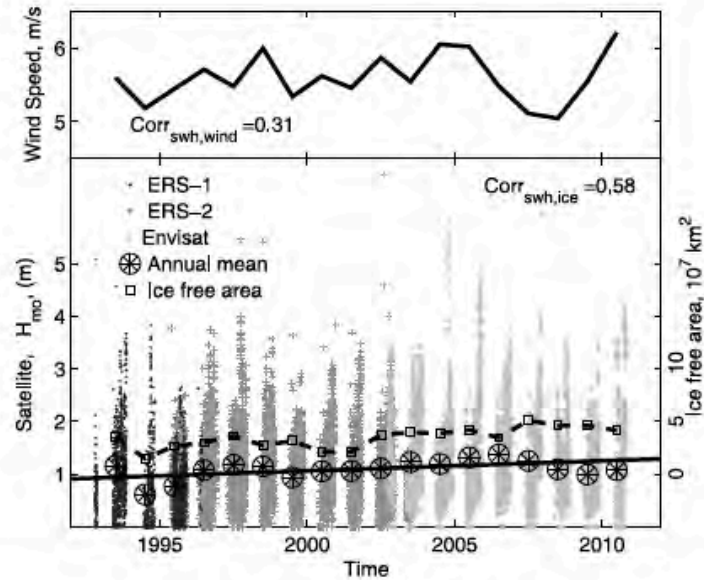


Figure 3. Significant wave height (SWH) for the period 1993–2010 for the southeast Chukchi Sea around Station 2007 (i.e., largest domain around Station 2007 in Figure 1) showing (top) NCEP NCAR Reanalysis I wind [Kistler *et al.*, 2001] trend and correlation to SWH. (bottom) Satellite data and its mean value (stars) with solid line showing SWH mean trend. Dashed line is the ice-free area over the Chukchi Sea (Lat 65–74°N, Lon 170–210°E) for the period May 1 – Nov 1 for each year [Comiso and Nishio, 2008], and the correlation of sea ice concentration to SWH. The linear fit to the satellite data has a positive increment of 0.02 m/year with 80% and 90% confident intervals 0.008–0.03 m/year and 0.005–0.033 m/year, respectively.

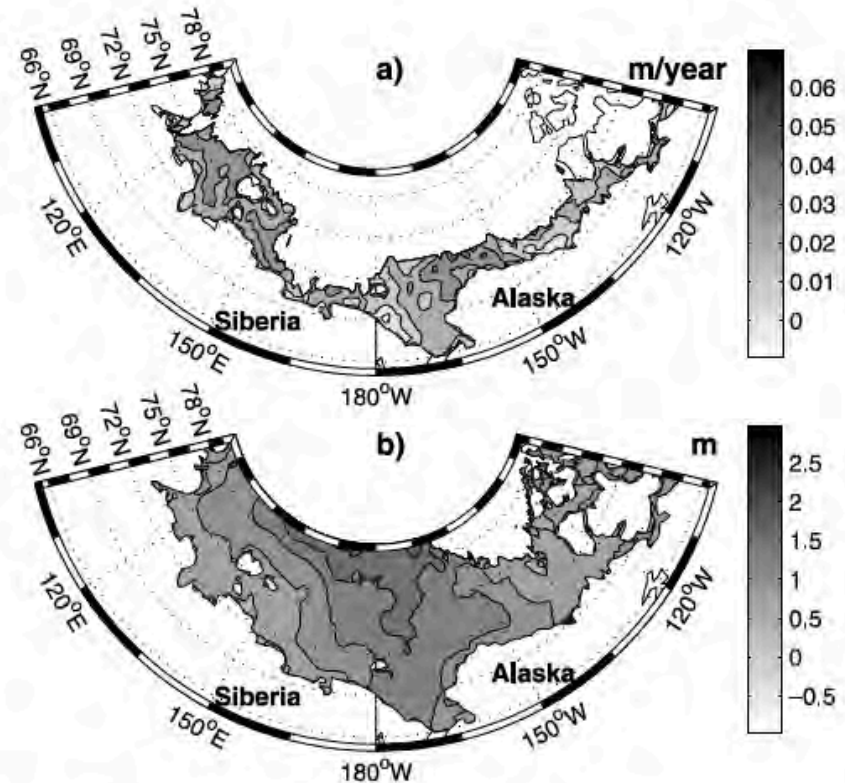
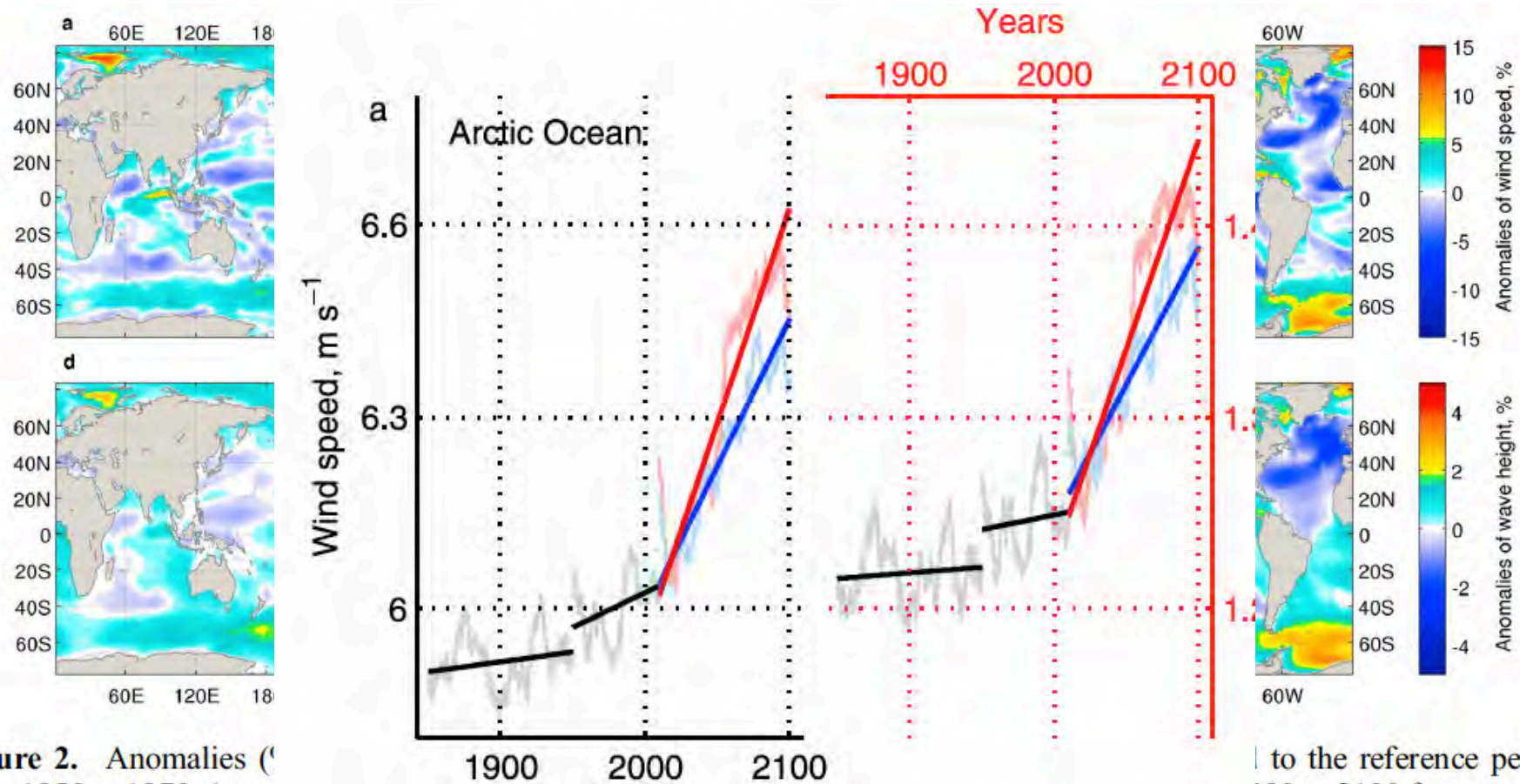


Figure 4. Significant wave height (SWH) for the period 1993–2010 for Pacific-Arctic region showing (a) SWH incremental change (m/year) and, (b) SWH mean value.



CMIP5 experiments, no ice

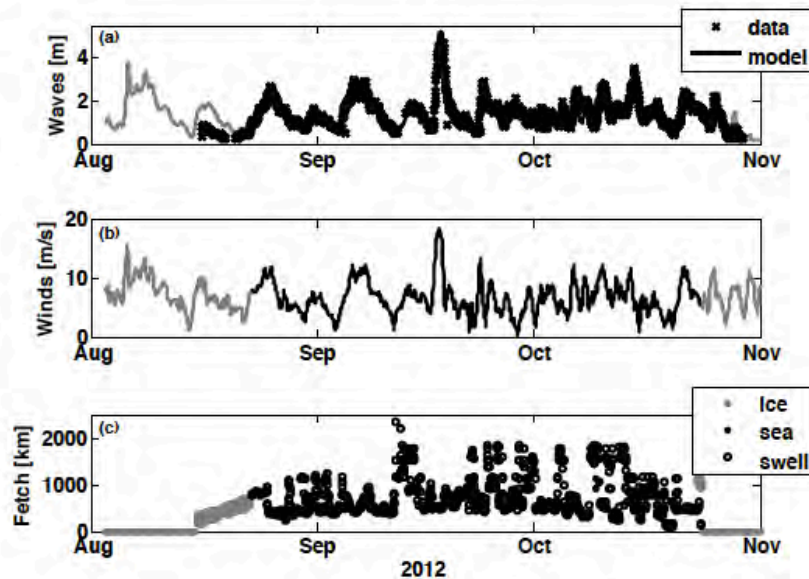


Figure 2. Time series of Arctic Ocean wave conditions. Hourly values for (a) significant wave height, (b) wind speed at 10 m reference height, and (c) fetch along the direction of the wind, from the mooring location to ice or land. In (a), symbols show the in situ observations, and the solid curve shows the model hindcast results. Gray is used to indicate the presence of partial ice cover (as determined from the mooring data). In (c), filled symbols are for wave conditions that are pure wind seas and open symbols are for wave conditions that include swells (as determined by non-dimensional wave age, $\frac{c}{U}$).

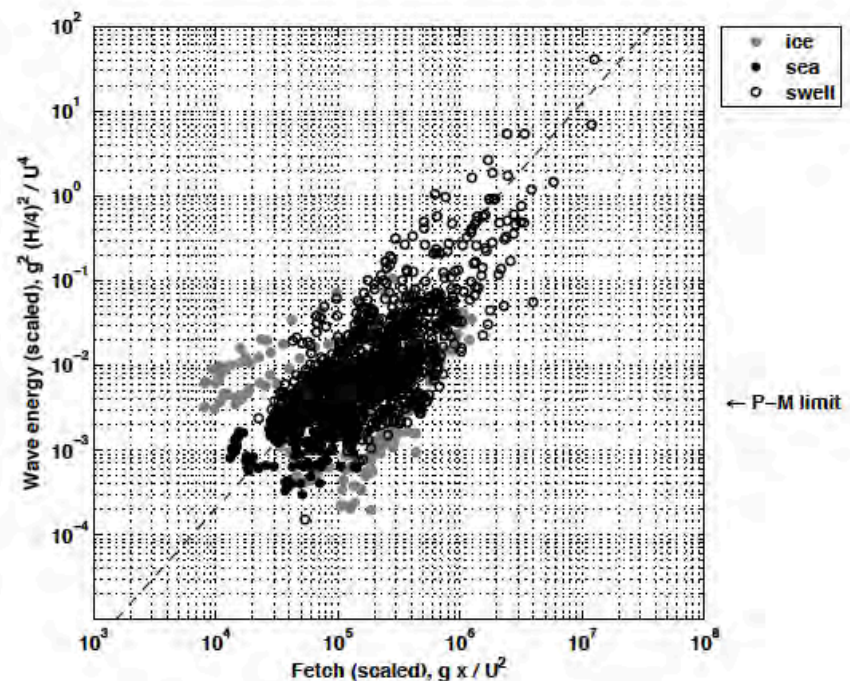


Figure 3. Scaling of waves in the Arctic Ocean, using non-dimensional wave energy versus non-dimensional fetch. There are 1880 points (each corresponding to an hourly observation from the in situ mooring at 75° N, 150° W). Symbols as in Figure 2. The dashed line is a regression with a logarithmic slope of 1.6. The Pierson-Moskowitz limit for pure wind seas is shown at $\mathcal{E} = 3.64 \times 10^{-3}$.